0026-895X/88/060779-14$02.00/0

MOLECULAR PHARMACOLOGY, 34:779–792

^{125}I-Neuropeptide Y and ^{125}I-Peptide YY Bind to Multiple Receptor Sites in Rat Brain

MARY W. WALKER and RICHARD J. MILLER

Department of Pharmacological and Physiological Sciences, University of Chicago, Chicago, Illinois 60637

Received June 30, 1988; Accepted September 6, 1988

SUMMARY

We describe the preparation of monoiodinated neuropeptide Y (Tyr^1-^{125}I-NPY) and monoiodinated peptide YY (Tyr^{36}-^{125}I-PYY). Using these ligands, we detected high, moderate, and low affinity receptor populations in rat brain. Only high and moderate affinity binding sites were suggested by saturation binding studies. Tyr^1-^{125}I-NPY bound to 8 ± 3% of the sites with a K_d of 54 pM (B_{max} = 19.4 fmol/mg of protein) and to 92 ± 3% of the sites with a K_d of 0.92 nM (B_{max} = 220.0 fmol/mg of protein). Tyr^{36}-^{125}I-PYY bound to 14 ± 3% of the sites with a K_d of 23.5 pM (B_{max} = 36.4 fmol/mg of protein) and to 86 ± 3% of the sites with a K_d of 1.9 nM (B_{max} = 220.1 fmol/mg of protein). The fragments NPY 13–36 and PYY 13–36 were able to compete with 10 pM Tyr^1-^{125}I-NPY for essentially all the binding sites. The fragments were 1 to 2 orders of magnitude less potent than the native peptides. Approximately 50% of the moderate affinity sites, but not the high affinity sites, were reversibly "lost" in the presence of 5′-guanylyl imidophosphate [Gpp(NH)p], a nonhydrolyzable analog of GTP. Kinetic studies revealed that Tyr^1-^{125}I-NPY dissociation could be best described by three dissociation rates. The proportions of slow and intermediate dissociation matched the proportions of moderate and high affinity binding sites, respectively, as suggested by equilibrium studies. There also existed a phase of fast dissociation. When Gpp(NH)p was added during dissociation, the proportion of slow dissociation decreased to the same extent that the fast dissociation was increased. However, the proportion of intermediate dissociation did not change. We propose that rat brain contains a minor population of high affinity NPY binding sites with an intermediate dissociation rate and no sensitivity to Gpp(NH)p. There is also a major population of moderate affinity binding sites with a slow dissociation rate. A component of these sites can convert to a low affinity state with a fast dissociation rate. Gpp(NH)p enhances conversion by stabilizing the low affinity state, thereby producing a "loss" of moderate affinity binding.

NPY is a 36-amino acid peptide neurotransmitter that is widely distributed throughout the central and peripheral nervous systems and also the adrenal gland (1–3). NPY is a member of the pancreatic polypeptide family, which also includes PYY and PP. In contrast to NPY, PYY has been localized mainly to the gastrointestinal mucosa (1, 2, 4), although relatively small amounts of authentic PYY have also been detected in the lower brainstem, spinal cord, hypothalamus, and median eminence of rat (5, 6). The highly conserved sequence homology shared by NPY and PYY is consistent with the similarity of their physiological effects (7, 8). These include vasoconstriction (9–11), regulation of feeding behavior (12, 13), and modulation of intestinal ion transport (14–16). Other effects are described in reviews (17, 18). NPY and PYY have been proposed to interact with a common receptor site (19, 20).

Functional studies with peripheral tissues provide support for the existence of NPY receptor subtypes. Postsynaptic NPY receptors have been shown to vasoconstrict several blood vessels in the rabbit and guinea pig (21–23). Postsynaptic NPY receptors on rabbit blood vessels have also been shown to potentiate the effects of other vasoconstrictors such as norepinephrine, histamine, and prostaglandin $F_{2\alpha}$ (21–23). Presynaptic NPY receptors have been shown to inhibit the release of neurotransmitters from peripheral nerve terminals. Some examples of this presynaptic effect include the inhibition of norepinephrine release from rat and mouse vas deferens (24, 25), the inhibition of norepinephrine release from rat perivascular sympathetic fibers (26, 27), the inhibition of acetylcholine release from rat cervix and the canine cardiac vagus (28, 29), and the inhibition of substance P release from rat DRG cells in culture (30). The C-terminal fragments NPY 13–36 and PYY 13–36 were found to be inactive at certain postsynaptic sites but mimicked the effects of NPY and PYY at presynaptic receptors in vas deferens (22, 23). Thus, certain peripheral

This work was supported by Public Health Service Grants DA-02121, DA-02575, and MH-40165 and by grants from Miles Pharmaceuticals and Marion Labs. M.W.W. was supported by Public Health Service Training Grant GM-07151. We are grateful to Dr. Howard S. Tager for his assistance with the synthesis of radioiodinated NPY and PYY.

ABBREVIATIONS: NPY, neuropeptide Y; PYY, peptide YY; PP, pancreatic polypeptide; Gpp(NH)p, 5′-guanylyl imidodiphosphate; ^{125}I-BH-NPY, ^{125}I-Bolton Hunter-NPY, ^{125}I-*N*-succinimidyl 3-(4-hydroxy 5-iodophenyl propionate NPY; DRG, dorsal root ganglion; HPLC, high performance liquid chromatography; BSA, bovine serum albumin; HEPES, *N*-2 hydroxyethyl-piperazine-*N*′-2-ethanesulfonic acid.

post- and presynaptic receptors are suggested to be structurally distinct. In a recent proposal, they have been classified as Y_1 and Y_2, respectively (31); NPY 13–36 and PYY 13–36 appear to be selective for Y_2 receptors (22, 23).

In analogy with the observed peripheral effects, NPY potentiated noradrenergic release of melatonin in rat pineal gland (32), α_2-adrenergic inhibition of [^{3}H]norepinephrine in rat hypothalamus (33), and α_2-adrenergic inhibition of [^{3}]norepinephrine in synaptosomes isolated from rat medulla oblongata (34). Adrenergic modulation was also observed in the form of receptor regulation. Short incubations with NPY modified the binding characteristics of α_2-adrenergic receptors in the rat medulla oblongata (35–37). Likewise, incubation with NPY induced up-regulation of α_1-adrenergic receptors in rat cerebral cortex; PYY 13–36 was ineffective (38). The central effects also include presynaptic inhibition of neurotransmitter release. NPY inhibited the release of [^{3}H]norepinephrine in the pineal gland, hypothalamus, and nucleus of the solitary tract from rat (32, 33, 39). The concept of Y_1 and Y_2 receptors was further developed by biochemical studies in cerebral cortex, where NPY inhibited adenylate cyclase activity and stimulated inositol phosphate hydrolysis. NPY 13–36 inhibited adenylate cyclase activity but had no effect on inositol phosphate hydrolysis (40).

Given the multiplicity of physiological effects and pharmacological evidence for receptor subtypes, one might expect to find evidence for heterogeneity in receptor binding studies. In agreement with this expectation, ^{125}I-PYY binding studies in porcine brain have indicated the existence of two receptor populations (20). However, with the exception of a report that [^{3}H]propionyl-NPY binds to high and low affinity sites in brain slices (41), studies in brain to date have been consistent with a one-site binding model. This is based on studies with ^{125}I-NPY (42–44), ^{125}I-BH-NPY (45–50), and [^{3}H]propionyl-NPY (47, 51). Some authors have remarked that nonlinear logarithmic plots of NPY dissociation from brain receptors provide evidence for heterogeneity (42, 45), but distinct receptor populations in brain have not been characterized in detail.

In the present series of studies, we describe the preparation of several ^{125}I-labeled forms of NPY and PYY and their use in the demonstration of multiple types of binding sites in rat brain. The relationship of these sites to the proposed NPY receptor heterogeneity is discussed.

Materials and Methods

Preparation of ^{125}I-NPY and ^{125}I-PYY. ^{125}I was incorporated into tyrosine using the chloramine T method. Phosphate buffer (0.25 M), pH 7.5 (40 μl), and 11.2 nmol of NPY or PYY (112 μl) were added to a vial containing 2 mCi (1 nmol of Na^{125}I (20 μl). The iodination was initiated by the addition of 72 nmol of chloramine T (40 μl) and was allowed to proceed for 1 min at 22°. The reaction was stopped with the addition of 1050 nmol sodium metabisulfite (100 μl) delivered in a 1-ml syringe. The contents of the vial were then drawn up into the syringe and transferred to a 12 × 75 mm test tube containing a 1-ml volume of Sephadex QEA-A25 anion exchange gel, which had been equilibrated and layered with 1 ml of the following buffer; 0.08 M Trizma base, 0.08 M NaCl, 0.02 M HCl, and 0.02% BSA, pH 8.6. [The Sephadex gel had been pretreated with a 1-ml solution of BSA (100 mg/ml), incubated with intermittent vortexing for 10 min, then allowed to settle for 10 min. The supernatant was removed, 1 ml of fresh buffer was added to the gel, and the procedure was repeated. The gel was rinsed with fresh buffer in this manner five times.] The iodinated peptide was extracted from the Sephadex gel in batch rinses as described for the BSA pretreatment. The rinses were pooled and centrifuged at 12,000 × g for 20 min to pellet out any accompanying Sephadex gel. The supernatant was acidified with glacial acetic acid to pH 3.5.

The peptides were subjected to a reverse phase HPLC purification scheme that included both gradient and isocratic modes. The HPLC components consisted of a Perkin-Elmer Series 4 liquid chromatograph, an Altex C-18 Ultrasphere ion-pairing column (5-μm particle size, 0.46 × 25 cm), and a mobile phase composed of acetonitrile and an aqueous buffer, 0.10 M phosphoric acid, 0.02 M triethylamine, 0.05 M $NaClO_4$, all brought to pH 3.0 with NaOH. Fractions of 0.5 ml were collected in 12 × 75 mm glass test tubes at a flow rate of 1 ml/min at 22°. The test tubes were pretreated with 10 μl of a 1% BSA solution to minimize the binding of the peptide to the glass.

Retention of the peptides on the column was optimized by employing a short gradient to an isocratic plateau over a period of 10 min. When NPY was injected onto the column, the acetonitrile was increased from 22 to 34% over the first 10 min and then maintained at 34% for 60 min; the iodinated peptide peaks eluted between 45 and 55 min. The procedure was similar for PYY except that the acetonitrile was increased from 20 to 30.4% over the first 10 min and then maintained at 30.4% for 60 min. The eluent was monitored for protein, as indicated by tyrosine absorbance at 278 nm, in a flow-through Perkin-Elmer LC-65T spectrophotometric detector. Fractions were counted for ^{125}I in a γ counter. The fractions corresponding to the major iodinated peptide peaks were pooled and concentrated under vacuum, then desalted at 4° on a Bio-gel P-2 gel filtration column (75 × 2.5 cm) equilibrated with 0.01 M Trizma-HCl, 0.1% BSA, and 0.02% sodium azide, pH 7.4. Fractions of 5 ml were collected in 13 × 100 mm test tubes at a flow rate of 1 ml/min and counted for ^{125}I. The fractions corresponding to the peptide peak were pooled, concentrated under vacuum, and stored at −20° until needed for experiments. The peptide solutions were always shell frozen in a bath of acetone and dry ice to avoid freeze-thaw damage.

Tryptic digestion. This was done to determine which of the five tyrosines in a particular fraction of HPLC-purified ^{125}I-NPY or ^{125}I-PYY was iodinated. The tryptic digestion products are amino acids 1–19 (Tyr^1), 20–25 (Tyr^{20} and Tyr^{21}), 26–35 (Tyr^{27}), and 36 (Tyr^{36}). A total of 100,000 cpm of the iodinated peptide was combined with 100 μg of trypsin in buffer, 0.01 M Trizma·HCl, 5 mM $CaCl_2$, pH 8.0. The reaction mixture (400 μl) was incubated in a shaking water bath for 1 hr at 37°. Tyrosine (0.5 mg) was then added to serve as a molecular weight marker. Unlabeled NPY or PYY (10 μg) was also added to minimize loss of the labeled peptide during gel filtration. The solution was applied to a Bio-gel P-4 gel filtration column equilibrated with a buffer containing 3 M acetic acid and 0.005% BSA at 4°. ^{125}I-NPY was applied to a 92 × 1 cm column; fractions of 0.625 ml were collected in 13 × 100 mm test tubes at a flow rate of 2 ml/hr. ^{125}I-PYY was applied to a 30 × 0.6 cm column; fractions of 0.475 ml were collected in 13 × 100 mm test tubes at a flow rate of 0.66 ml/min. The fractions were monitored for ^{125}I- in a γ counter and for tyrosine absorbance at 278 nm in a spectrophotometer. The elution volumes for the tryptic iodinated fragments were then compared with the elution volumes for the native iodinated peptides and for free tyrosine in order to estimate the molecular weights.

Membrane preparation. Adult female Holtzman Sprague-Dawley rats were decapitated and the brains were removed. The forebrain (the entire brain except the cerebellum and brainstem) was dissected out and transferred to ice-cold 0.32 M sucrose. The brain was homogenized in a glass tube with a loose-fitting Teflon pestle for 10–12 strokes and centrifuged at 800 × g for 10 min. The supernatant was reserved on ice, the pellet was rehomogenized in 0.32 M sucrose, and the homogenate was centrifuged at 800 × g for 10 min. The two supernatants were then centrifuged at 17,000 × g for 20 min. The resultant crude mitochondrial pellets were suspended in binding buffer, 137 mM NaCl, 5.4 mM KCl, 0.44 mM KH_2PO_4, 1.26 mM $CaCl_2$, 0.81 mM $MgSO_4$, 20 mM HEPES, 1 mM dithiothreitol, 0.1% bacitracin, 0.3% BSA, 100 mg/liter streptomycin sulfate, 1 mg/liter aprotinin, 10 mg/liter soybean trypsin inhibitor, and 1 μM captopril, pH 7.4. Ten milliliters of buffer were added to

the pellets for every gram of wet brain weight to produce a solution of approximately 2 mg/ml protein. The solution was homogenized with a loose-fitting Teflon pestle for three strokes to achieve an even suspension. The membranes were diluted 1:5 to produce a solution that, upon dilution during the binding assay, yielded a final protein concentration of approximately 0.2 mg/ml. Membranes were stored on ice.

Protein concentrations were measured according to the method of Bradford, using Bio-Rad reagent (52).

Binding experiments. Plastic microfuge tubes (1.5 ml) were filled with binding buffer, iodinated ligand, and other relevant reagents so that the total volume was 500 μl. Iodinated ligand was generally present in concentrations up to 100,000 cpm/ml (approximately 35–45 pM). To achieve greater concentrations, the iodinated peptide was diluted with unlabeled peptide. This manipulation is based on the assumption that both peptides bind to the receptors with similar affinity. Binding was initiated by adding 500 μl of membranes and vortexing. Tubes were incubated in a shaking water bath at 22°. The binding was terminated by centrifuging at 10,000 × *g* for 15 sec in a Beckman microfuge, aspirating the supernatant, rinsing the top of the pellet with ice-cold binding buffer, and aspirating again. The tip of the microfuge tube containing the pellet was cut off, dropped into a 12 × 75 mm test tube, and counted for ^{125}I in a γ counter.

Nonspecific binding for association curves was determined in the presence of 1×10^{-7} M NPY. For saturation binding studies, ligand concentrations ranged from 1×10^{-13} M to 3×10^{-8} M; nonspecific binding was determined by regression analysis (see below).

Dissociation experiments were performed by allowing the membranes to preincubate with radioligand (total volume, 950 μl) for 1 hr at 22° (equilibrium conditions). Dissociation rates were measured by the addition of 2×10^{-6} M NPY (50 μl), which was subsequently diluted to 1×10^{-7} M NPY. The binding was terminated by microcentrifugation (10,000 × *g* for 15 sec) at various time points over a 3-hr period. Nonspecific binding was measured at the beginning and end of the dissociation phase using membranes exposed to 1×10^{-7} M NPY during the entire preincubation period (total volume, 1000 μl). As the nonspecific binding was virtually constant, the two measurements were averaged and subtracted from total binding.

Peptide stability. The structural stability of ^{125}I-NPY was analyzed by gel filtration. ^{125}I-NPY (4×10^6 cpm) was incubated with membranes (0.2 mg of protein/ml) for 1 hr at 22°. The bound ligand was separated from the free ligand by microcentrifugation. The bound ligand was extracted from the pellet with 3 M acetic acid (950 μl). An aliquot of free ligand (25 μl) was added to fresh membranes (0.2 mg of protein/ml) suspended in 3 M acetic acid (950 μl), vortexed 1 min, and separated by microcentrifugation at 10,000 × *g* for 1 min. This step was necessary to inactivate and/or remove acid-sensitive proteases that accompanied the free ligand. The samples were then applied to a Bio-gel P-4 gel filtration column (92 × 1 cm) equilibrated with 3 M acetic acid and 0.005% BSA at 4° and analyzed for proteolysis as described in the procedure for tryptic digestion.

Data analysis and statistics. Saturation binding curves plotted as bound ligand versus free ligand were interpreted as having both specific (*s*) and nonspecific (*ns*) components according to an adsorption isotherm model, in which the amount of radioligand associated with a population of binding sites at equilibrium (B_{eq}) is related to the entire population of binding sites (B_{max}) by the ligand concentration [*L*] and the dissociation constant K_d:

$$B_{eq} = \frac{B_{max,\,s} \cdot [L]}{[L] + K_{d,\,s}} + \frac{B_{max,\,ns} \cdot [L]}{[L] + K_{d,\,ns}}$$

Nonspecific binding was defined as binding for which $K_d \gg [L]$, so that the binding sites are not saturated within the range of ligand concentrations used in the analysis. The adsorption isotherm for nonspecific binding is therefore reduced to a linear term, where C_1 and C_2 refer to the slope and intercept, respectively:

$$B_{eq} = \frac{B_{max,\,s} \cdot [L]}{[L] + K_{d,\,s}} + C_1 \cdot [L] + C_2$$

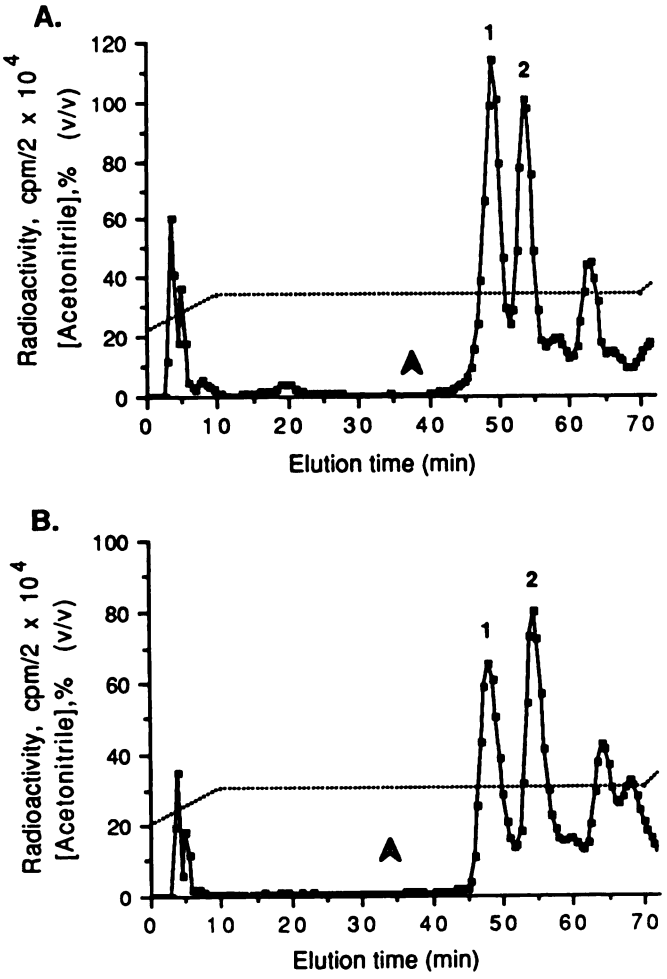

Fig. 1. HPLC purification of ^{125}I-NPY (A) and ^{125}I-PYY (B). The peptides were iodinated and purified as described in Materials and Methods. *Arrows* mark the elution of the uniodinated peptide. *Dotted lines* indicate the percentage of acetonitrile.

In this case, the term "nonspecific" reflects a mathematical relationship between binding site and ligand without assigning functional status. This technique was employed because 1) it minimized error associated with the calculation of specific binding for each individual point, 2) it allowed a description of the data with the least number of transformations, and 3) it conserved materials.

Binding experiments were analyzed with a modified version of a nonlinear least squares regression routine encoding a simplex algorithm (53, 54). Adsorption isotherms and kinetic models used to describe binding data were based on one or more additive and independent binding sites. Linear transformations of the data were avoided, except in the calculation of Hill slope parameters. "Goodness-of-fit" was indicated by the sum of squares ($SS = \sum (y_i - \mu(x_i))$, where y_i and $\mu(x_i)$ correspond to the actual *y* value and the predicted *y* value, respectively). The descriptive value of a model as applied to a particular set of data was assessed by comparing the associated sum of squares with that of other possible models and obtaining an *F* statistic (55).

Data are reported as the mean ± standard error. Where appropriate, significance levels were determined using the two-tailed Student's *t* test. A p value ≤ 0.05 was considered statistically significant.

Materials. Porcine NPY, porcine PYY, GTP sodium salt, Gpp(NH)p, and L-1-tosylamide-2-phenylethyl chloromethyl ketone-treated trypsin were purchased from Sigma (St. Louis, MO). ^{125}I was purchased from Amersham (Arlington Heights, IL). Porcine NPY 13–36 and porcine PYY 13–36 were the kind gift of Claes Wahlestedt. All

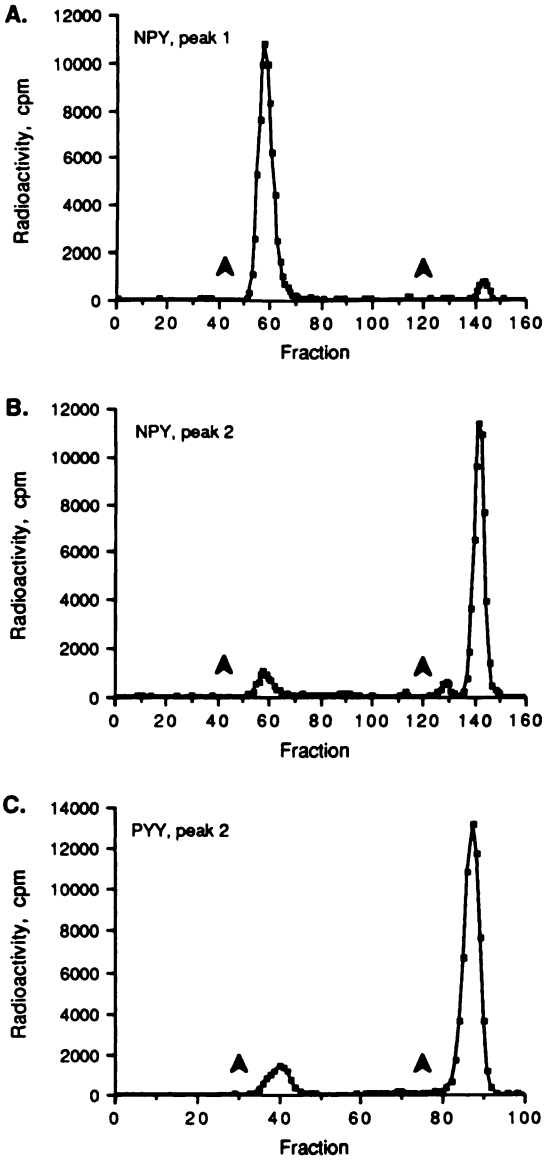

Fig. 2. Tryptic digestion of selected ligands. A, Elution profile of trypsin-digested ^{125}I-NPY, HPLC peak 1. B, Elution profile of trypsin-digested ^{125}I-NPY, HPLC peak 2. C, Elution profile of trypsin-digested ^{125}I-PYY, HPLC peak 2. *White arrows* represent the elution of undigested peptide. *Black arrows* represent the elution of free tyrosine. Each elution profile is representative of two experiments.

other materials were reagent grade or higher and were obtained from standard sources.

Results

Synthesis of ^{125}I-NPY and ^{125}I-PYY. Reverse phase HPLC allowed the separation of various iodinated isomers of ^{125}I-NPY and ^{125}I-PYY from the uniodinated peptide (Fig. 1). Both peptides yielded similar chromatograms, with two prominent peaks (peaks 1 and 2) and at least one lesser peak eluting during the isocratic phase.

The two major peaks were collected and analyzed for their ability to bind specifically to rat brain membranes. ^{125}I-NPY eluted from the reverse phase HPLC column at a higher percentage of acetonitrile than did ^{125}I-PYY, suggesting that ^{125}I-NPY was more hydrophobic and might therefore be expected to produce more nonspecific binding. This was in fact observed.

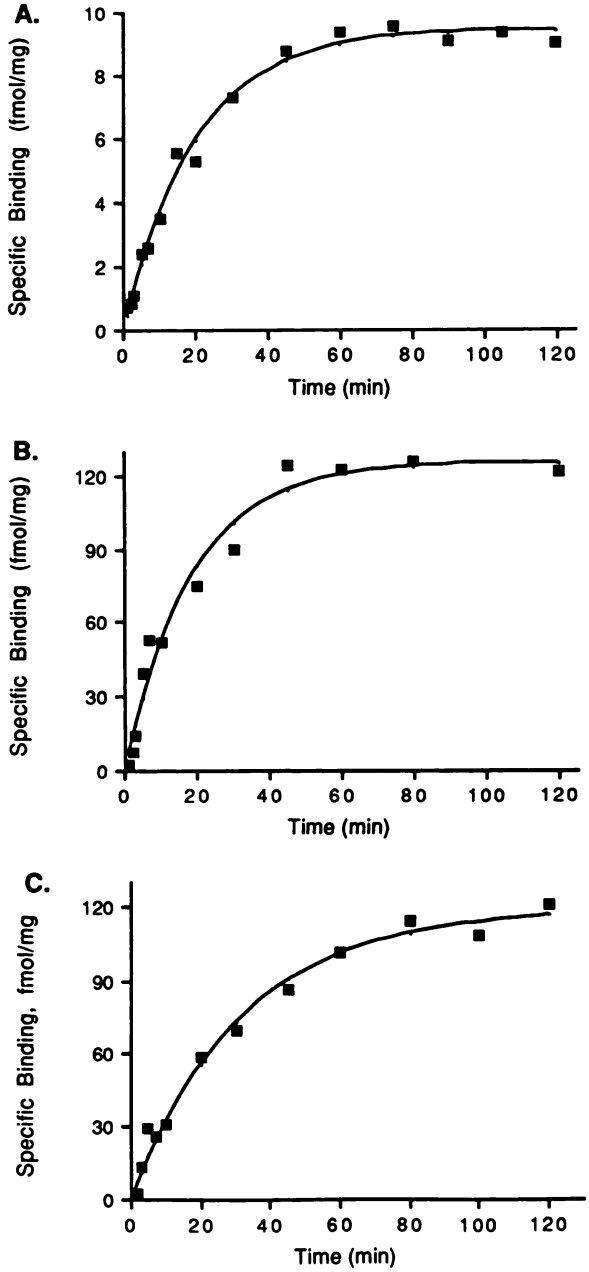

Fig. 3. Time course of association at 22°. A, Initial concentration, 23 pM Tyr^1-^{125}I-NPY. B, Initial concentration, 1 nM Tyr^1-^{125}I-NPY. C, Initial concentration, 1 nM Tyr^{36}-^{125}I-PYY. Experiments were performed in duplicate five times with 23 pM Tyr^1-^{125}I-NPY, in triplicate four times with 1 nM Tyr^1-^{125}I-NPY and in triplicate three times with 1 nM Tyr^{36}-^{125}I-PYY; representative experiments are shown.

When iodinated peptide (20,000 cpm) was incubated with membranes with or without 1×10^{-7} M NPY for 60 min at 22°, nonspecific binding of ^{125}I-NPY relative to total binding was 20% (peak 1) and 24% (peak 2), whereas nonspecific binding of ^{125}I-PYY was 5% (peak 1) and 8% (peak 2; data not shown). Both synthetic yield from the reverse phase HPLC column and nonspecific binding to membranes were considered in order to select a choice peak for use in all subsequent experiments. Peak 1 was selected in the case of ^{125}I-NPY, whereas peak 2 was selected in the case of ^{125}I-PYY.

The location of the ^{125}I-tyrosine within the selected peptides was determined by tryptic digestion (Fig. 2). The potential

TABLE 1

Binding parameters for Tyr^1-^{125}I-NPY and Tyr^{36}-^{125}I-PYY to rat brain membranes

The data were fit by one- or two-site adsorption isotherm models with additive and independent terms, as described in Materials and Methods. B_{max} is reported in fmol/mg protein. The one-site model included a total of four parameters for K_d, B_{max}, C_1 (slope), and C_2 (intercept). The two-site model included an additional two parameters for the second K_d and B_{max}. Parameters are listed for the two-site model. SS_1 and SS_2 refer to the sums of squares for the one-site and two-site models, respectively. All experiments were done in triplicate, four experiments for Tyr^{36}-^{125}I-PYY, three experiments for all other conditions.

	K_{d1}	B_{max1}	K_{d2}	B_{max2}	SS_1	SS_2
	pM	fmol/mg of protein	nM	fmol/mg of protein		
Tyr^1-^{125}I-NPY	54.1 ± 32.6	19.4 ± 8.8	0.92 ± 0.34	220.0 ± 5.7	111.4 ± 78.2	107.3 ± 79.0
Tyr^1-^{125}I-NPY + Gpp(NH)p	97.4 ± 35.6	22.8 ± 12.4	1.7 ± 1.4	81.2 ± 6.1[a]	158.2 ± 145.1	154.0 ± 141.2
Tyr^{36}-^{125}I-PYY	23.5 ± 6.5	36.4 ± 9.2	1.9 ± 0.66	220.1 ± 22.5	192.2 ± 78.9	84.4 ± 37.0
Tyr^{36}-^{125}I-PYY + Gpp(NH)p	33.4 ± 3.2	30.0 ± 2.9	1.0 ± 0.17	126.5 ± 5.4[b]	98.3 ± 44.5	65.9 ± 31.5

[a] Unpaired Student's t test for B_{max2} with or without Gpp(NH)p, $p < 0.001$.
[b] $p < 0.018$.

tryptic fragments are amino acids 1–19 (Tyr^1), 20–25 (Tyr^{20} and Tyr^{21}), 26–35 (Tyr^{27}), and 36 (Tyr^{36}). Tryptic digestion of ^{125}I-NPY (peak 1) yielded an iodinated fragment with an estimated molecular weight of 2100 Da, corresponding to fragment 1–19. Therefore, this ligand is more accurately described as Tyr^1-^{125}I-NPY. For comparison, tryptic digestion of ^{125}I-NPY (peak 2) yielded an iodinated fragment with an estimated molecular weight of 100 Da, corresponding to a single amino acid. Therefore, this ligand was identified as Tyr^{36}-^{125}I-NPY. A similar pattern was observed for ^{125}I-PYY (peak 2), which was identified as Tyr^{36}-^{125}I-PYY.

Associated with each peptide was a minor component representing contamination from the adjacent peak on the HPLC column. When Tyr^1-^{125}I-NPY was digested, for example, approximately 5% of the radioactivity eluted in the position of Tyr^{36}-^{125}I. Alternatively, when Tyr^{36}-^{125}I-PYY was digested, approximately 10% of the radioactivity eluted in the position of 1–19 (Tyr^1-^{125}I). Because the conclusions in this study depend largely on results obtained using ^{125}I-NPY, the IC_{50} for NPY binding was determined with both Tyr^1-^{125}I-NPY and Tyr^{36}-^{125}I-NPY. The IC_{50} with 10 pM Tyr^1-^{125}I-NPY was 0.37 ± 0.058 nM and the IC_{50} with 10 pM Tyr^{36}-^{125}I-NPY was 0.40 ± 0.067 nM; the difference was statistically insignificant (data not shown).

The specific activities obtained by calculation were typically in the range of 35–45 fmol/100,000 cpm. The calculation is based on two assumptions. The first is that each iodinated peptide molecule had incorporated 1 atom of ^{125}I. Although this was not determined by a direct method such as mass spectometry or atomic absorption, the assumption is justified for the following reasons. 1) Tryptic digestion indicated that each selected peptide contained a single iodinated tyrosine. 2) The ratio of ^{125}I to peptide in the iodination reaction was 1:11.4, thereby favoring monoiodinated tyrosine.

The second assumption is that the iodinated peptides were fully separated from uniodinated peptide. Absorbance spectrophotometry indicated that the unlabeled peptide eluted from the HPLC column before peak 1 (Fig. 1). Given that there was some cross-contamination between adjacent radioactive peaks, it is possible that peak 1 was contaminated to some extent with uniodinated peptide. The error associated with the specific activity would then be proportional to the extent of contamination. A small error in specific activity, however, would not alter the intrinsic ability of the ligand to distinguish between receptor subtypes, and thus, no further corrections were made.

Time course of equilibrium binding. The time course of NPY binding at 22° was studied at initial concentrations of 23 pM and 1 nM Tyr$^{1-125}$I-NPY (Fig. 3, A and B). In both cases, receptor binding reached equilibrium within 60 min. The observed association constant (k_{obs}) was 0.051 ± 0.004 min^{-1} with 23 pM Tyr^1-^{125}I-NPY (five experiments) and 0.055 ± 0.01 min^{-1} with 1 nM Tyr^1-^{125}I-NPY (four experiments). The corresponding $t_{1/2}$ values were 14.0 ± 1.1 min and 14.7 ± 3.7 min, respectively.

For comparison, the time course of Tyr^{36}-^{125}I-PYY binding was measured at 1 nM ligand concentration (Fig. 3C). The k_{obs} = 0.029 ± 0.002 min^{-1}; $t_{1/2}$ = 24.3 ± 1.3 min (three experiments).

Ligand stability. The extent of peptidergic degradation during equilibrium binding studies was measured by gel filtration. Previous studies have indicated that an amidated tyrosine at the carboxy terminus of NPY is critical for receptor activation (22, 23, 40, 56–58). Although different effects have been reported depending upon the receptor under study, the receptor activation process generally appears less vulnerable to modifications of the amino terminal residues (22, 23, 58–60).

To examine degradation from either terminus, both Tyr^1-^{125}I-NPY and Tyr^{36}-^{125}I-NPY were incubated with membranes for 60 min at 22°, as in a typical equilibrium binding experiment. The bound ligand was separated from the free ligand, and each pool was applied separately to a gel filtration column. In every case, 95% or more of the radioactivity eluted in the position of intact ^{125}I-NPY (data not shown). The elution pattern for Tyr^1-^{125}I-NPY revealed that the peptide was cleaved to a small extent. The iodinated fragment had an approximate molecular weight of 1700 Da, indicating that proteolysis occurred in the vicinity of Pro^{13}-Ala^{14}. The elution pattern for Tyr^{36}-^{125}I-NPY revealed that the peptide was also cleaved to a small extent near the carboxy terminus. The iodinated fragments had approximate molecular weights of 1000 Da and less, indicating that the region from Asn^{29} to Tyr^{36} was susceptible to proteolysis.

Equilibrium binding studies. Both high and moderate affinity receptor populations were suggested by analysis of saturation binding at equilibrium (Table 1). A two-site model consistently provided the better fit, as indicated by the residual sum of squares. The F statistic did not consistently yield a p value ≤ 0.05 in all experiments, such that the characterization of binding sites from saturation studies alone was inconclusive. However, the characteristics of the two-site model were upheld by dissociation studies (see below). The two-site model was therefore considered for its descriptive value. According to the two-site model, Tyr^1-^{125}I-NPY bound to 8 ± 3% of the sites with high affinity (K_{d_1} = 54 ± 33 pM, B_{max_1} = 19.4 ± 8.8 fmol/

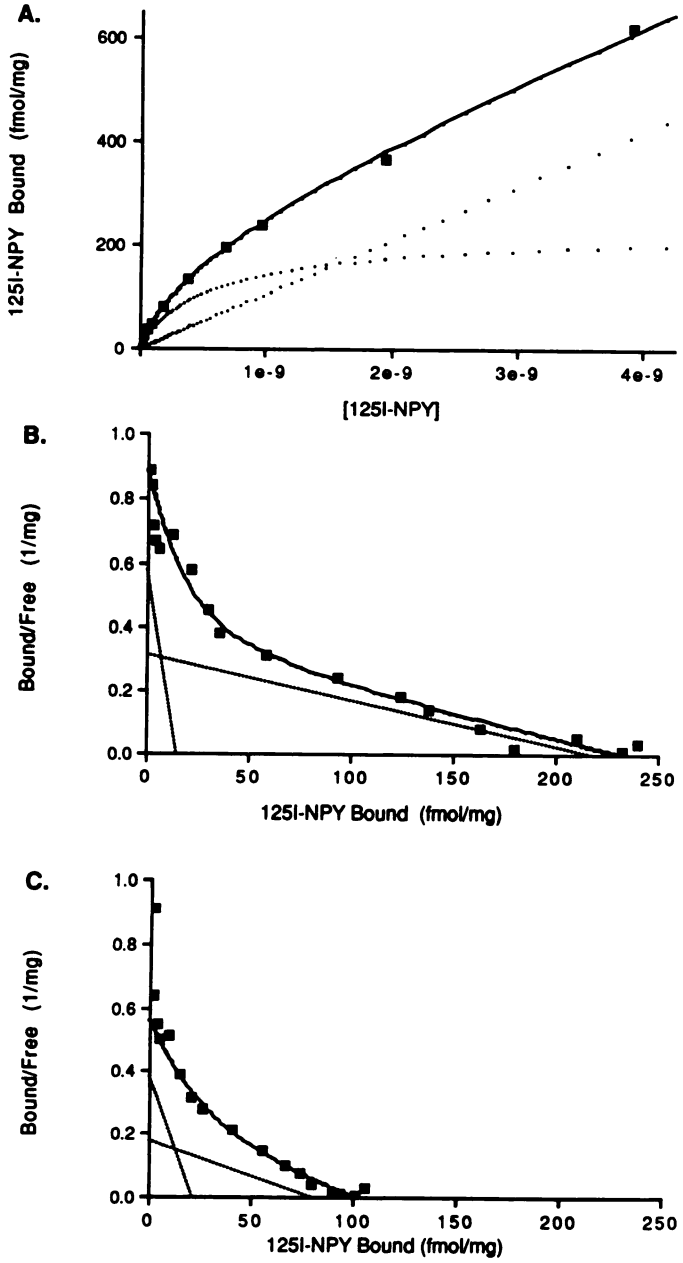

Fig. 4. Saturation binding curves with Tyr^{1}-^{125}I-NPY. A, Total binding. Detail is plotted from experiments in which ligand concentration ranged from 1×10^{-13} M to 3×10^{-8} M. *Dotted lines* represent specific (saturating) and nonspecific (nonsaturating) binding as determined by nonlinear least squares analysis. B, Specific binding from A was transformed into Scatchard coordinates for graphical display. C, Specific binding in the presence of 1×10^{-4} M Gpp(NH)p, transformed into Scatchard coordinates. Experiments were performed in triplicate three times; representative experiments are shown.

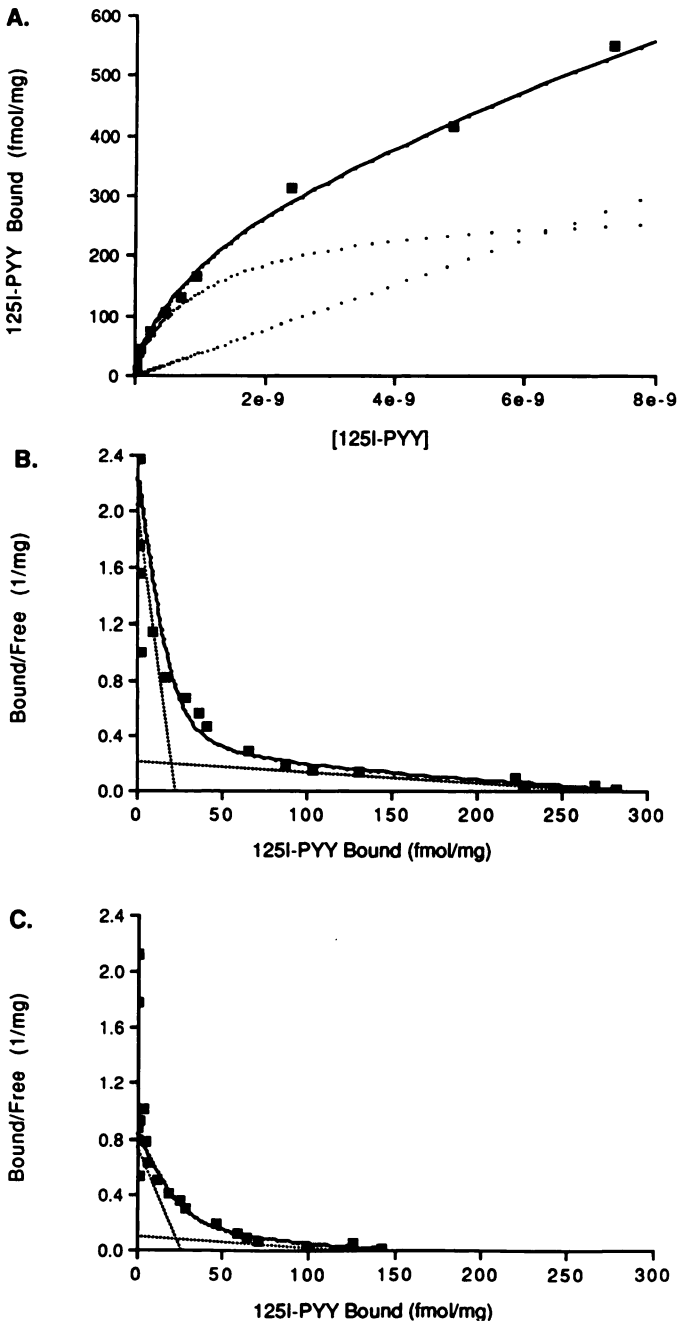

Fig. 5. Saturation binding curves with Tyr^{36}-^{125}I-PYY. A, Total binding. Detail is plotted from experiments in which ligand concentration ranged from 1×10^{-13} M to 3×10^{-8} M. *Dotted lines* represent specific (saturating) and nonspecific (nonsaturating) binding as determined by nonlinear least squares analysis. B, Specific binding from A was transformed into Scatchard coordinates for graphical display. C, Specific binding in the presence of 1×10^{-4} M Gpp(NH)p, transformed into Scatchard coordinates. Experiments were performed in triplicate four times for control membranes and three times for membranes + Gpp(NH)p; representative experiments are shown.

mg of protein) and to 92 ± 3% of the sites with moderate affinity (K_{d_2} = 0.92 ± 0.34 nM, B_{max_2} = 220.0 fmol/mg of protein) (Fig. 4, A and B). These parameters are similar to those reported for ^{125}I-NPY binding to DRG cells (30). Tyr^{36}-^{125}I-PYY bound to 14 ± 3% of the sites with high affinity (K_{d_1} = 23 ± 7 pM, B_{max_1} = 36.4 ± 9.2 fmol/mg of protein) and to 86 ± 3% of the sites with moderate affinity (K_{d_2} = 1.9 ± 0.66 nM, B_{max_2} = 220.1 fmol/mg) (Fig. 5, A and B). Thus, both Tyr^{1}-^{125}I-NPY and Tyr^{36}-^{125}I-PYY appeared to detect heterogeneous populations of binding sites in brain. As the apparent K_d values for Tyr^{36}-^{125}I-PYY were relatively farther apart, Tyr^{36}-^{125}I-PYY seemed to be more capable of discriminating between heterogeneous sites under these conditions.

NPY receptor binding in brain has been shown to be reduced by guanine nucleotides with little or no change in affinity (43, 45, 47, 49). We wondered whether binding was reduced in both the high and moderate affinity populations suggested by the

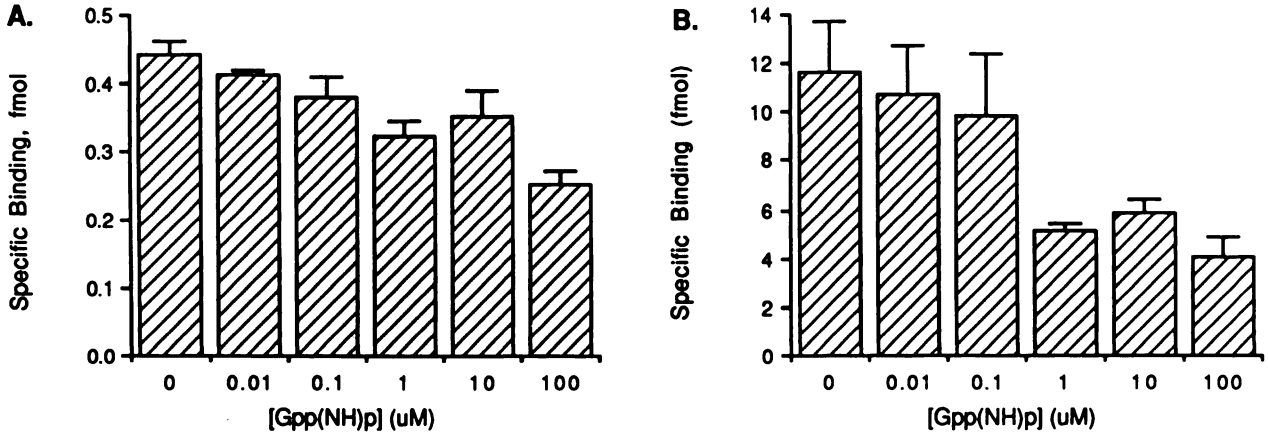

Fig. 6. Concentration-response curve for Gpp(NH)p effects on Tyr^{36}-^{125}I-PYY binding. A, 8 pM Tyr^{36}-^{125}I-PYY. B, 1 nM Tyr^{36}-^{125}I-PYY. Gpp(NH)p exerted half-maximal effects at approximately 3×10^{-7} M. Each *point* represents a triplicate determination; average values are shown. Based on these results, [Gpp(NH)p] = 1×10^{-4} M when used in subsequent experiments.

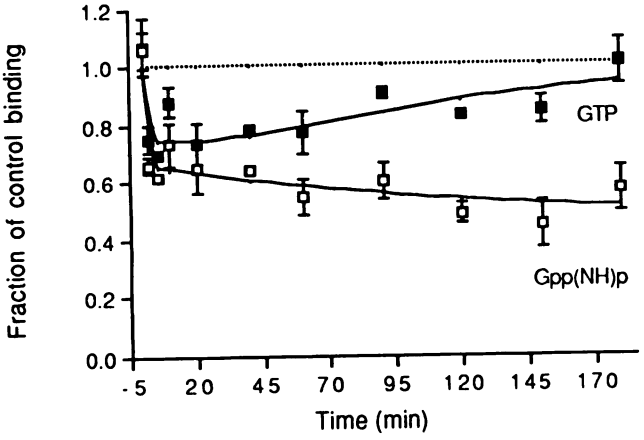

Fig. 7. Reversibility of guanine nucleotide effects. Membranes were divided into three groups and incubated with 30 pM Tyr^{1}-^{125}I-NPY for 60 min at 22° (total reaction volume, 12 ml). At that point (time = 0 on the *abscissa*), the membranes were transferred to a 37° water bath. A 1-ml sample was withdrawn to measure the equilibrium binding. The membranes were then supplemented with 111 μl of GTP, final concentration, 1×10^{-6} M (■); Gpp(NH)p, final concentration, 1×10^{-4} M (□); or plain buffer (· · ·). Aliquots were withdrawn from each group at the indicated times. Specific binding was calculated and reported as the fraction of control specific binding. The experiment was performed in singlicate three times; average values are shown.

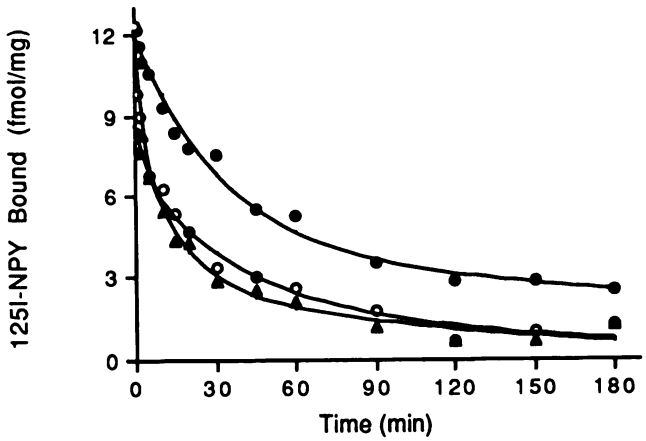

Fig. 8. Dissociation with 32 pM Tyr^{1}-^{125}I-NPY. Membranes were preincubated with radioligand for 60 min at 22°. The dissociation period was initiated by the addition of 1×10^{-7} M NPY. The three curves are control membranes (●), membranes that received 1×10^{-4} M Gpp(NH)p at the 0 time point of dissociation (○), and membranes that received 1×10^{-4} M Gpp(NH)p at the start of the incubation (▲). The experiment was performed in singlicate three times; a representative experiment is shown.

saturation curves. In preliminary experiments, we measured the ability of Gpp(NH)p, a nonhydrolyzable analog of GTP, to reduce Tyr^{36}-^{125}I-PYY binding at 8 pM and 1 nM ligand concentrations (Fig. 6). Gpp(NH)p reduced the binding in both cases with a half maximal effect at approximately 3×10^{-7} M and a maximal effect at 1×10^{-4} M. The potency of Gpp(NH)p was in agreement with the earlier reports (43, 45, 47, 49). However, the maximum effect was smaller at 8 pM Tyr^{36}-^{125}I-PYY than at 1 nM Tyr^{36}-^{125}I-PYY. Inasmuch as the high affinity receptors were preferentially occupied at 8 pM ligand, it appeared that the proposed high affinity receptors were relatively less sensitive to guanine nucleotides.

Scatchard plots of equilibrium binding curves in the presence of Gpp(NH)p are presented in Fig. 4C and Fig. 5C. As suggested by the Gpp(NH)p dose-response curves, the moderate affinity binding observed with the two-site binding model was reduced approximately 60% with Tyr^{1}-^{125}I-NPY and 40% with Tyr^{36}-^{125}I-PYY. There was no significant difference in B_{max_1}, K_{d_1}, or K_{d_2} for the remaining sites.

With regard to ligand binding, the most commonly documented effect of guanine nucleotides is to induce a conversion of receptors from a high affinity state to a low affinity state without changing the binding capacity. It is therefore somewhat surprising that guanine nucleotides reduced the binding capacity of NPY receptors with no apparent change in K_d. However, there are other peptide receptors that exhibit a similar response (61, 62). The observed change in B_{max} raises some interesting questions about the mechanism of receptor regulation. For example, one could imagine that the GTP-sensitive receptors are removed from the total pool by mechanisms such as cleavage, endocytotic internalization, or phosphorylation. A more simplistic explanation is that guanine nucleotides induce such a large shift in K_d that the receptors only appear to be lost. Such a loss would be observed if ligand concentrations were not large enough to saturate the receptors in their new low affinity state. Even if a portion of the low affinity receptors were labeled, the binding might be difficult to detect by equilib-

TABLE 2

Dissociation parameters with 32 pM Tyr¹-¹²⁵I-NPY

Control refers to membranes that were incubated with radioligand for 60 min and then supplemented with 1×10^{-7} M NPY. Gpp(NH)p refers to membranes that were incubated with radioligand and 1×10^{-4} M Gpp(NH)p for 60 min and then supplemented with 1×10^{-7} M NPY plus 1×10^{-4} M Gpp(NH)p. Control/Gpp(NH)p refers to membranes that were incubated with radioligand for 60 min and then supplemented with 1×10^{-7} M NPY plus 1×10^{-4} M Gpp(NH)p. The data were fit by one-, two-, or three-site dissociation models with additive and independent terms ($B = B_{eq}(e^{-k_{-1} \cdot t})$, as described in Materials and Methods. The one-site model included a total of two parameters for B_{eq} and k_{-1}. The two- and three-site models included an additional two and four parameters, respectively. Parameters are listed for the three-site model. SS_1, SS_2, and SS_3 refer to the sums of squares for the one-, two-, and three-site models, respectively. The sums of squares were derived for bound values as cpm uncorrected for [protein]. The bound values were subsequently converted to fmol of Tyr¹-¹²⁵I-NPY/mg of protein. Average values are presented from experiments performed three times in singlicate.

	Intermediate		Slow		Fast		SS_1	SS_2	SS_3
	Rate	Number	Rate	Number	Rate	Number			
	min^{-1}	fmol/mg	min^{-1}	fmol/mg	min^{-1}	fmol/mg			
Control	0.0428	6.27	0.00549	7.25	0.345	2.10	3634628	473004	317926
SE	0.0098	1.07	0.00075	1.44	0.107	0.17	899519	136114	141788
Gpp(NH)p	0.127	6.78	0.00929	4.57	0.345	0.00	2074032	326987	326987
SE	0.044	1.39	0.00061	0.91	0.106	0.00	452067	58125	58125
Control/Gpp(NH)p	0.0427	5.93	0.00651	3.55	1.336	5.16	5203656	1027693	461056
SE	0.00611	0.96	0.00042	0.59	0.65	0.77	866819	422280	32385

rium binding assays. This is because the majority of binding was nonspecific at ligand concentrations greater than 5 nM Tyr¹-¹²⁵I-NPY and 20 nM Tyr³⁶-¹²⁵I-PYY (Figs. 4A and 5A); the signal to noise ratio was proportionally decreased.

To investigate this last possibility, we reasoned that allosteric conversion to a low affinity state in a membrane preparation would be readily reversible. Three groups of membranes were incubated with Tyr¹-¹²⁵I-NPY to reach equilibrium at 22°. The membranes were then treated with an aliquot of Gpp(NH)p, GTP, or plain buffer and incubated at 37°; the temperature was raised to facilitate the hydrolysis of GTP. Aliquots were withdrawn from each group at various time points over the course of 3 hr in order to compare the levels of specific binding (Fig. 7). Gpp(NH)p induced a persistent loss of binding compared with control levels. GTP, however, induced an initial loss, which began to reverse after 20 min; specific binding was nearly identical to control levels after 180 min. The reversible effect of GTP is consistent with a model in which guanine nucleotides allosterically convert a component of the moderate affinity receptor population to a low affinity state.

Dissociation experiments. The heterogeneity of the NPY binding sites was further explored using dissociation experiments. If the dissociation curves were composed of multiple phases described by distinct off-rates, one would predict that the proportions of these phases should correspond in some way to the proportions of receptor populations derived from equilibrium binding experiments. Using the equilibrium-derived K_d and B_{max} values for Tyr¹-¹²⁵I-NPY, the proportions of high and moderate affinity receptor populations were calculated for three concentrations of ligand, 10 pM (56% high, 44% moderate), 32 pM (50% high, 50% moderate), and 0.95 nM (15% high, 85% moderate). These three ligand concentrations were then used to construct a family of dissociation curves.

In support of the equilibrium binding studies, the dissociation curves obtained with 32 pM Tyr¹-¹²⁵I-NPY were better described by a two-site model than a one-site model, as indicated by the sums of squares (Fig. 8; Table 2). The F statistic yielded a p value ≤ 0.001 in all experiments (three experiments). However, the data were best described by three distinct off-rates, which will be referred to as slow (0.00549 min^{-1}), intermediate (0.0428 min^{-1}), and fast (0.345 min^{-1}) (Fig. 8; Table 2). The F statistic for the two- and three-site models did not consistently yield a p value ≤ 0.05 in all experiments, such that the characterization of three binding sites from dissociation curves was inconclusive. However, the superiority of the three-site model led us to hypothesize that Tyr¹-¹²⁵I-NPY might recognize three receptor populations that could not be clearly resolved. Thus, we considered the three-site model for its descriptive value, with the intention of testing it in further dissociation studies. With respect to Tyr¹-¹²⁵I-NPY binding, 6.27 fmol/mg of protein dissociated at the intermediate rate and 7.25 fmol/mg of protein dissociated at the slow rate. Because it was predicted that the high and moderate affinity receptors should each represent approximately 50% of the binding at 32 pM Tyr¹-¹²⁵I-NPY, it seemed reasonable that these components of dissociation represented the proposed high and moderate affinity receptor populations. In addition, 2.10 fmol/mg of protein dissociated at the fast rate. Initially, this component did not appear to correspond in any obvious way to the receptor populations described by saturation curves.

To correctly identify the various components of the dissociation curve, it was necessary to determine which component was reduced in the presence of guanine nucleotides. Dissociation with 32 pM Tyr¹-¹²⁵I-NPY was therefore measured when Gpp(NH)p was present throughout the entire experiment, i.e., during the initial preincubation period and during the dissociation period (Fig. 8; Table 2). Again, the data were better described by the two-site model than by the one-site model. The F statistics yielded p values ≤ 0.003 in all experiments (three experiments). In contrast to the control experiments, the inclusion of Gpp(NH)p yielded data that were described equally well by the two-site and three-site models; the residual sum of squares was identical in either case. According to the two-site model, the Tyr¹-¹²⁵I-NPY dissociated at rates comparable to the intermediate and slow rates observed with the control membranes; the differences were statistically insignificant. With respect to Tyr¹-¹²⁵I-NPY binding, 5.93 fmol/mg of protein dissociated at the intermediate rate and 4.57 fmol/mg of protein dissociated at the slow rate. The component of intermediate dissociation was unchanged compared with the control membranes, whereas the component of slow dissociation was reduced by 2.68 fmol/mg of protein (37%). This is consistent with a model in which the component of slow dissociation corresponds to the moderate affinity, guanine nucleotide-sensitive binding site and the component of intermediate dissociation corresponds to the high affinity, guanine nucleo-

tide-insensitive binding sites. As compared with the control membranes, a measurable component of fast dissociation was conspicuously absent. Thus, the fast dissociation rate appeared to be associated with some type of guanine nucleotide-sensitive binding site.

Finally, we tested whether Gpp(NH)p-induced conversion of ligand-occupied moderate affinity receptors to the low affinity state had any effect on dissociation rates. Membranes were incubated with 32 pM Tyr^1-^{125}I-NPY to reach equilibrium, and Gpp(NH)p was added at the 0 time point of dissociation (Fig. 8; Table 2). As in the control experiments, the data were better described by a two-site than a one-site model. The *F* statistic yielded *p* values ≤ 0.003 in all experiments (three experiments). However, the data were again best fit by a three-site model. The *F* statistic for the two- and three-site models did not consistently yield a *p* value ≤ 0.05 in all experiments, such that the characterization of three binding sites was inconclusive. However, the superiority of the three-site model, especially in this paradigm, led us to consider the three-site model for comparison with the other dissociation studies. According to the three-site model, Tyr^1-^{125}I-NPY dissociated at rates comparable to the intermediate, slow, and fast rates observed with control membranes; the differences were statistically insignificant. With respect to Tyr^1-^{125}I-NPY binding, 6.78 fmol/mg of protein dissociated at the intermediate rate, 3.55 fmol/mg of protein at the slow rate, and 5.16 fmol/mg of protein dissociated at the fast rate. The component of intermediate dissociation was unchanged compared to control experiments, whereas the component of slow dissociation was reduced by 3.70 fmol/mg of protein (51%). The component of fast dissociation was increased by 3.01 fmol/mg of protein. This pattern of dissociation provides further support for a model in which the component of intermediate dissociation represents high affinity, guanine nucleotide-insensitive receptors and the component of slow dissociation represents moderate affinity, guanine nucleotide-sensitive receptors. In addition, the component of fast dissociation coincides descriptively with the low affinity sites, a portion of which are thought to be newly converted from moderate affinity state in the presence of Gpp(NH)p. If the fast component in this condition is equivalent in nature to the fast component observed with the control membranes, it is conceivable that the moderate affinity sites equilibrate with the low affinity state in the absence of guanine nucleotides.

If the dissociation curve can be described by a three-site model, and if the intermediate and slow off-rates are correctly assigned to the high and moderate affinity binding site populations, then the proportion of sites dissociating at the intermediate and slow off-rates should be a predictable function of ligand concentration. Because the high affinity binding sites are selectively occupied at low ligand concentrations, this model predicts that the proportion of intermediate dissociation (proposed high affinity sites) should be greatest at low ligand concentrations. Conversely, the proportion of slow dissociation (proposed moderate affinity sites) should be greatest at large ligand concentrations. To confirm this relationship, the same curves were derived using 10 pM Tyr^1-^{125}I-NPY and 0.95 nM Tyr^1-^{125}I-NPY. The analysis at different concentrations yielded patterns similar to those observed with 32 pM Tyr^1-^{125}I-NPY (Fig. 9; Table 3). In all cases, the slow component was diminished when Gpp(NH)p was present throughout the entire experiment. The addition of Gpp(NH)p at the 0 time point of

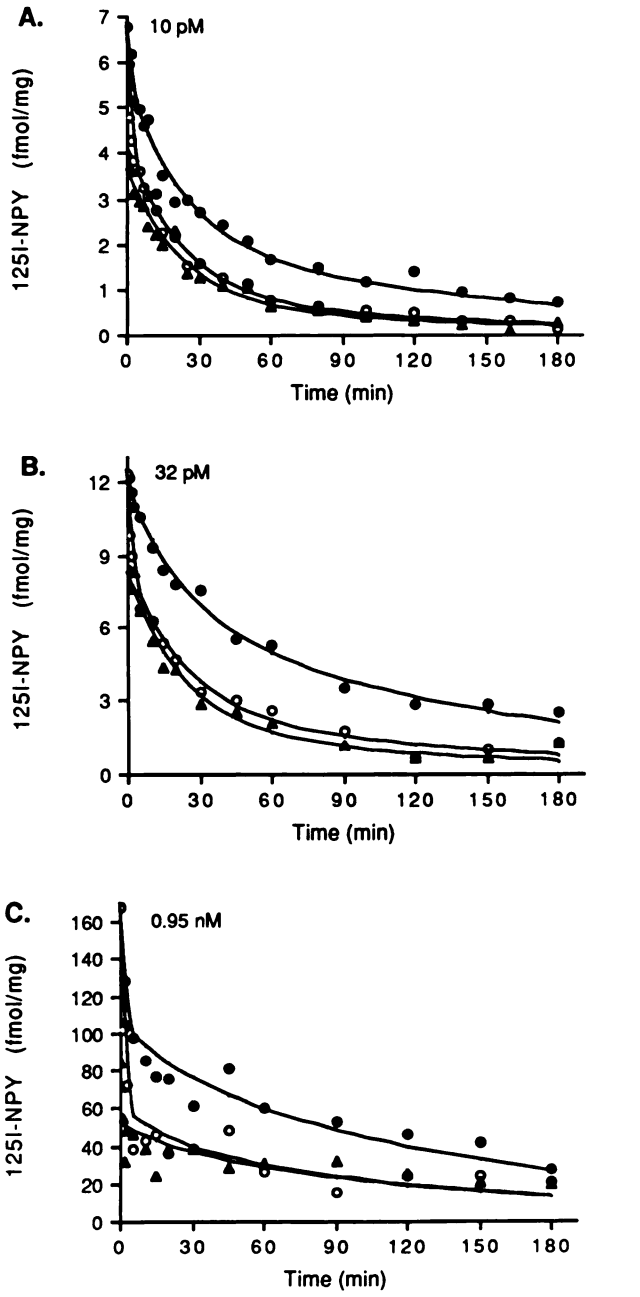

Fig. 9. Dissociation curves with 10 pM (A), 32 pM (B), and 0.95 nM Tyr^1-^{125}I-NPY (C) and constrained off-rates for a three-site model. Dissociation experiments were performed as described in the legend to Fig. 8. The ability of the three-site model to describe the dissociation was tested by fixing the rates at representative intermediate, slow, and fast values and determining whether the proportions of sites dissociating at those rates varied in a predictable fashion. The representative off-rates were obtained from experiments in which Gpp(NH)p was added at the 0 time point of dissociation to membranes equilibrated with 32 pM Tyr^1-^{125}I-NPY (fast off-rate = 1.336 min^{-1}), intermediate off-rate = 0.0427 min^{-1}, and slow off-rate = 0.00651 min^{-1}; Table 2), because the sums of squares indicated that the three-site model was most clearly distinguished from the two-site model in that case. The components dissociating at each representative rate were then derived using nonlinear regression analysis. The three curves for each ligand concentration are control membranes (●), membranes that received 1×10^{-4} M Gpp(NH)p at the 0 time point of dissociation (○), and membranes that received 1×10^{-4} M Gpp(NH)p at the start of the incubation (▲). The experiments were performed in singlicate three times; representative experiments are shown.

TABLE 3

Dissociation parameters with fixed rates

Control refers to membranes that were incubated with radioligand for 60 min and then supplemented with 1×10^{-7} M NPY. Gpp(NH)p refers to membranes that were incubated with radioligand and 1×10^{-4} M Gpp(NH)p for 60 min and then supplemented with 1×10^{-7} M NPY plus 1×10^{-4} M Gpp(NH)p. Control/Gpp(NH)p refers to membranes that were incubated with radioligand for 60 min and then supplemented with 1×10^{-7} M NPY plus 1×10^{-4} M Gpp(NH)p. The data were fit by a three-site dissociation model with additive and independent terms ($B = B_{\infty}(e^{-(k-1)\cdot t})$, as described in Materials and Methods. The rates were fixed at 0.0427 min^{-1} (intermediate), 0.00651 min^{-1} (slow), and 1.336 min^{-1} (fast) (see Fig. 9 legend). The components dissociating at each rate are reported as fmol of Tyr^1-^{125}I-NPY/mg of protein; average values are presented from experiments performed three times in singlicate.

	Dissociation								
	10 pM Ligand			32 pM Ligand			0.95 nM Ligand		
	Intermediate	Slow	Fast	Intermediate	Slow	Fast	Intermediate	Slow	Fast
	fmol/mg of protein								
Control	3.05	2.49	1.11	6.63	7.51	1.51	16.60	72.39	41.34
SE	0.74	0.24	0.17	1.40	0.65	0.50	1.68	6.98	12.03
Gpp(NH)p	2.64	0.82[a]	0.00[g]	7.31	2.38[c]	0.00[i]	13.70	34.40[e]	0.00[k]
SE	0.21	0.29	0.00	1.15	0.44	0.00	1.82	3.27	0.00
Control/Gpp(NH)p	2.86	1.02[b]	2.74[h]	7.41	3.35[d]	4.84[j]	15.41	33.98[f]	82.06[l]
SE	0.32	0.18	0.36	1.25	0.50	0.88	1.95	4.89	15.66

Unpaired Student's *t* test with respect to the control component of slow dissociation: [a] $p < 0.011$; [b] $p < 0.007$; [c] $p < 0.003$; [d] $p < 0.007$; [e] $p < 0.008$; [f] $p < 0.011$. With respect to the control component of fast dissociation: [g] $p < 0.003$; [h] $p < 0.015$; [i] $p < 0.039$; [j] $p < 0.030$; [k] $p < 0.008$; [l] $p < 0.108$.

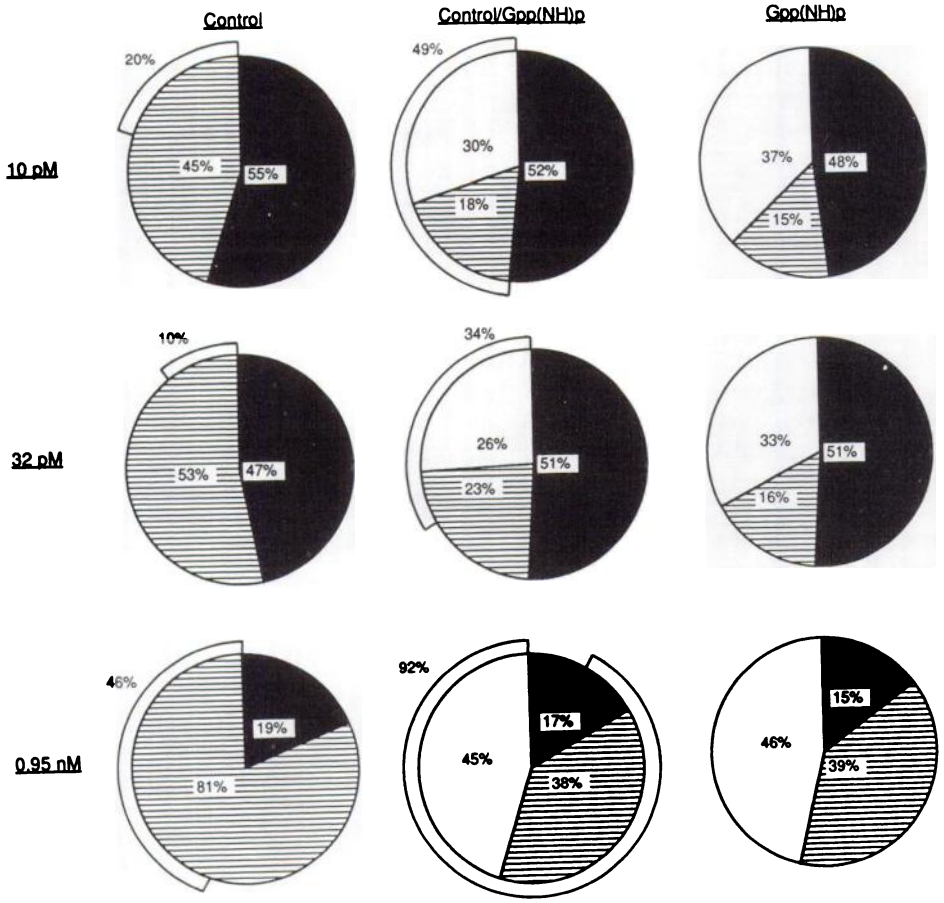

Fig. 10. Distribution of binding sites dissociating at intermediate, slow, and fast constrained off-rates with 10 pM, 32 pM, and 0.95 nM Tyr^1-^{125}I-NPY. The data from Fig. 9 and Table 3 are transformed for graphical display. The distribution is described for control membranes (*Control*), membranes that received 1×10^{-4} M Gpp(NH)p at the 0 time point of dissociation [*Control/Gpp(NH)p*], and membranes that received 1×10^{-4} M Gpp(NH)p at the start of the incubation [*Gpp(NH)p*]. Percentages are calculated with respect to the combined components of intermediate and slow dissociation observed in control membranes. The intermediate off-rate is represented by a *black sector*, the slow off-rate is represented by a *striped sector*, and a loss of binding sites compared with the control membranes is represented by a *white sector*. The fast dissociation relative to the combined total of intermediate and slow dissociation is represented by a *band* around the perimeter. The experiments were performed in singlicate three times; average values are shown.

dissociation reduced the component of slow dissociation by approximately 50%. The difference was made up by an increase in the component of fast dissociation. When the components were expressed as a percentage of the combined intermediate and slow dissociation measured in control membranes, the relationships predicted by the equilibrium binding parameters were readily apparent (Fig. 10). In the presence of 10 pM Tyr^1-^{125}I-NPY, the component of intermediate dissociation was 55% and the component of slow dissociation was 45%; this agrees with the predicted ratio of 56% high affinity and 44% moderate affinity receptors. With 32 pM Tyr^1-^{125}I-NPY, the component of intermediate dissociation was 47% and the component of slow dissociation was 53%; this agrees with the predicted ratio of 50% high affinity and 50% moderate affinity receptors. With 0.95 nM Tyr^1-^{125}I-NPY, the component of intermediate dissociation was 19% and the component of slow dissociation was 81%; this agrees with the predicted ratio of 15% high affinity and 85% moderate affinity receptors. Because the receptor populations can be matched in terms of proportion and guanine nucleotide sensitivity without the inclusion of the fast component, it seems possible that the fast dissociation rate is associated with a nonsaturating pool of binding sites that was con-

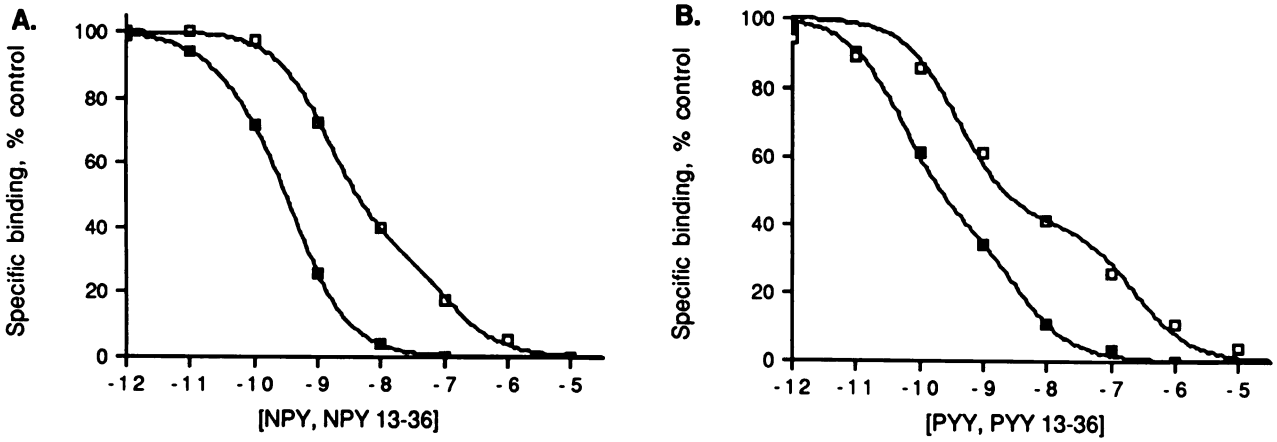

Fig. 11. Competition curves with 10 pM Tyr^1-^{125}I-NPY and fragments. A, The competing peptides were NPY (■) and NPY 13–36 (□). B, The competing peptides were PYY (■) and PYY 13–36 (□). The experiments were performed in triplicate three times; representative experiments are shown.

sidered nonspecific by the nonlinear least squares regression routine described in Material and Methods. In other words, the dissociation experiments may have revealed the existence of a low affinity, guanine nucleotide-sensitive binding site that escaped detection in saturation binding experiments.

Fragment binding. Investigations with NPY 13–36 and PYY 13–36 have led to the proposal that both peripheral and central NPY receptor populations contain subtypes, Y_1 and Y_2, with the fragments selectively activating the Y_2 receptor (31). To determine whether the fragments bind selectively to the receptor populations observed in the present study, 10 pM Tyr^1-^{125}I-NPY was incubated with membranes so that the label was distributed over the high and moderate affinity sites with a predicted ratio of approximately 60–40. Both NPY 13–36 and PYY 13–36 were able to compete with the label for essentially all of the available sites (Fig. 11). In comparison with competition curves obtained with native peptides, the fragments were less potent by 1 to 2 orders of magnitude; the difference between the native peptides and the fragments increased at higher concentrations. The Hill slope for NPY 13–36 was 0.64 ± 0.03 (three experiments); the Hill slope for NPY under the same conditions was 0.81 ± 0.07 (five experiments).[1] The Hill slope for PYY 13–36 was 0.40 ± 0.02 (three experiments); the Hill slope for PYY under the same conditions was 0.59 ± 0.01 (four experiments).[1]

Discussion

With the use of the reverse phase HPLC purification scheme described, we were able to purify monoiodinated isomers of ^{125}I-NPY and ^{125}I-PYY with high specific activity and high affinity for binding sites in brain. Consistent with the sequence homology between both peptides, the elution patterns from the HPLC column were essentially identical. Similar chromatographic patterns have been reported for the HPLC purification of ^{125}I-NPY and ^{125}I-PP (60). Furthermore, the patterns can be interpreted with regard to tertiary structure in the pancreatic polypeptide family. X-ray crystallographic analysis has revealed that avian PP possesses a compact tertiary structure (63–66). The avian PP molecule contains a polyproline II-type helix in residues 2–8 and an amphiphilic α-helix in residues 14–32. The two helical regions are brought together by a type II β-bend in residues 9–12 and interdigitate via hydrophobic side chains. Circular dichroism studies indicate that the folded structure is stable even in dilute aqueous solution (63, 66, 67). This information, combined with knowledge of the sequence homology between avian PP and rat NPY, has led to a proposed structure for NPY based on computer modeling (68). All of the residues required for the maintenance of helix-helix interactions in avian PP are either conserved or replaced by homologous residues in NPY, such that the tertiary structures appear to be remarkably similar. The fact that the two most prominent peaks from the HPLC column in these studies corresponded to ^{125}I-Tyr^1 and ^{125}I-Tyr^{36} is consistent with a model in which the N- and C-terminal tyrosines are equally accessible to iodination in solution. Conceivably, the internal tyrosines are hidden within the helical structures during the iodination reaction.

The elution pattern from the HPLC column gave rise to the following rank order, starting with the earliest elution: PYY, Tyr^1-^{125}I-PYY, Tyr^{36}-^{125}I-PYY, NPY, Tyr^1-^{125}I-NPY, Tyr^{36}-^{125}I-NPY. The observed levels of nonspecific binding gave rise to the following rank order, starting with the lowest nonspecific binding: Tyr^1-^{125}I-PYY, Tyr^{36}-^{125}I-PYY, Tyr^1-^{125}I-NPY, Tyr^{36}-^{125}I-NPY. The elution pattern therefore appears to be correlated with hydrophobic interactions in the membrane preparation. From the viewpoint of hydrophobicity alone, it would seem advantageous to use the first iodinated peptide to elute from the column.

Other ligands beside Tyr^1-^{125}I-NPY offer unique advantages with regard to the investigation of the NPY receptor. The binding profiles obtained for Tyr^{36}-^{125}I-PYY and Tyr^1-^{125}I-NPY were qualitatively similar, supporting the proposal that both PYY and NPY interact with common receptor sites (19, 20). However, Tyr^{36}-^{125}I-PYY was able to discriminate between receptor populations more fully under these conditions, as indicated by the lower Hill slope and the greater difference between K_{d_1} and K_{d_2}.

It was also interesting to compare the fragments NPY 13–36 and PYY 13–36 with NPY and PYY. Although NPY 13–36 and PYY 13–36 were approximately 1 order of magnitude less potent than the native peptides in competing for the high affinity sites in brain, the difference increased as the low

[1] D. R. Lynch, M. W. Walker, R. J. Miller, and S. H. Snyder. Neuropeptide Y receptors in rat brain: differential autoradiographic localizations with [^{125}I]peptide YY and [^{125}I]neuropeptide Y imply receptor heterogenicity. Submitted.

affinity sites were occupied. The fragments also yielded Hill slopes that were lower than those for the native peptides. The results indicate that the fragments are better able to discriminate heterogeneity among receptor populations in brain.

Physiological assays have demonstrated that the fragments selectively mimic the effects of NPY at presynaptic (Y_2) receptors, which inhibit neurotransmitter release in the periphery. Furthermore, the fragments did not antagonize the effects of NPY at postsynaptic (Y_1) receptor in guinea pig vein and rabbit femoral artery (23). Thus, the evidence suggests that the fragments selectively bind and activate Y_2 receptors. NPY 13–36 and PYY 13–36 were able to compete for essentially all of the binding sites in brain accessible to Tyr^1-^{125}I-NPY. One interpretation, then, is that the majority of NPY receptors in the brain are the proposed Y_2 subtype.

However, the fragments are not able to mimic all of the effects of native NPY and PYY in brain. For example, NPY 13–36 did not stimulate inositol phosphate hydrolysis and PYY 13–36 did not upregulate α_1-adrenergic receptors in rat cerebral cortex (38, 40). Consequently, it is possible that Y_2 receptors can be further classified into subtypes, based on the ability to be activated by NPY 13–36 and PYY 13–36. Yet another consideration is that the fragments are not equally selective in various systems. For example, NPY 13–36 exerted postsynaptic vasoconstrictor effects in pig spleen with a 10-fold lower potency than NPY (58). NPY 16–36 and NPY 19–36 produced vasoconstriction in guinea pig heart *in vitro* (59). Also, NPY 13–36 stimulated inositol phosphate hydrolysis in cultured DRG cells while inhibiting the release of substance P (30, 69). Thus, generalizations about ligand specificity and receptor subtypes in different physiological systems must be made with caution.

The two K_d values we observed for Tyr^1-^{125}I-NPY in equilibrium binding studies are compared with K_d values reported by other authors using various NPY-derived radioligands in rat brain (Table 4). The range of reported K_d values extends from 10 pM to 1.8 nM. The differences between reported values could be due to several factors, including ligand characteristics, specific activity, membrane preparation, buffer composition, binding protocol, and data analysis. Yet another factor to consider is differential distribution of high and moderate affinity binding sites.[1] The predominant binding sites in the brain regions under study will influence the observed K_d. The binding parameters obtained with Tyr^{36}-^{125}I-PYY in our studies are also compared with those observed for ^{125}I-PYY in porcine hippocampus (Table 4). The K_d values reported for porcine hippocampus are relatively large; this could reflect species differences as well as the factors cited for Tyr^1-^{125}I-NPY binding.

TABLE 4

Comparison of binding parameters in brain

All binding parameters are reported for rat brain, except where indicated for ^{125}I-PYY.

Region	K_d	Reference	Radioligand
Forebrain	K_{d1}, 54 pM K_{d2}, 0.92 nM	Present study	Tyr^1-^{125}I-NPY
Forebrain	K_{d1}, 10 pM K_{d2}, 100 nM	41	[^{3}H]NPY
Whole brain − cerebellum	1.8 nM	51	[^{3}H]NPY
Whole brain − cerebellum	0.35 nM	44	^{125}I-NPY
Cerebral cortex	0.32 nM	43	^{125}I-NPY
Cerebral cortex	0.39 nM	47	^{125}I-BH-NPY
Cerebral cortex	0.53 nM	47	[^{3}H]NPY
Cerebral cortex	0.38 nM	42	^{125}I-NPY
Striatum	0.29 nM	42	^{125}I-NPY
Hippocampus	0.1 nM	45	^{125}I-BH-NPY
Hippocampus	0.09 nM	46	^{125}I-BH-NPY
Hippocampus	0.34 nM	42	^{125}I-NPY
Hypothalamus	0.34 nM	42	^{125}I-NPY
Lower brainstem	0.39 nM	49	^{125}I-BH-NPY
Forebrain	K_{d1}, 23 pM K_{d2}, 1.9 nM	Present study	Tyr^{36}-^{125}I-PYY
Hippocampus (pig)	K_{d1}, 139 pM K_{d2}, 37.2 nM	20	^{125}I-PYY

Tyr^1-^{125}I-NPY binding was clearly resolved into components in a dissociation paradigm. Biphasic dissociation curves from rat brain membranes have been reported for ^{125}I-NPY (initial off-rate = 0.0636 min^{-1}) (42) and ^{125}I-BH-NPY (off-rates = 0.033 min^{-1} and 0.0087 min^{-1}) (45). A "fast" dissociation rate has not been previously reported; this could reflect differences in binding protocol. For example, in the earliest study, the dissociation was measured at 37° and terminated by filtering the membranes and washing them three times (42). In the second study, the dissociation was measured at 37° and terminated by the addition of 1 ml of ice-cold buffer and microcentrifugation for 4 min (45). In either case, the component of fast dissociation might have been lost in the final step. Nonetheless, the reproducible pattern of multiple phases supports the proposal that NPY radioligands label multiple sites in brain. Furthermore, by analyzing the phases in terms of guanine nucleotide sensitivity, we were able to distinguish the various components and compare them with equilibrium binding populations. The data from the saturation studies and dissociation experiments were mutually supportive, thereby strengthening the case for receptor heterogeneity.

Investigations of NPY receptors in brain have led other authors to speculate why guanine nucleotides reduce the B_{max} without changing the K_d. Possible reasons include 1) GTP-induced desensitization, 2) strong negative cooperativity between agonist binding sites induced by heterologous interaction with GTP, and 3) two subpopulations of receptors, one of which is insensitive to guanine nucleotides and the other of which responds to guanine nucleotides with such a large loss in affinity that the sites cannot be labeled in equilibrium binding experiments (43). Clearly, this question can only be answered correctly when the relationship of the various receptor sites to one another is elucidated. For example, do the sites interact such that negative cooperativity is feasible in the presence of GTP? Is the guanine nucleotide-insensitive portion of the moderate affinity population physically distinct and unrelated to the guanine nucleotide-sensitive portion? Does the component of fast dissociation represent a physically distinct and unrelated low affinity receptor population that "disappears" in the presence of guanine nucleotides? Alternatively, does the component of fast dissociation reflect equilibration of the moderate affinity receptors with a low affinity state?

Although these possibilities cannot be distinguished at the present time, the data from the present study suggest that there is a minor population of high affinity sites with an intermediate dissociation rate and no measurable sensitivity to guanine nucleotides. There also exists a major population of moderate affinity sites with a slow dissociation rate; a component of these sites is sensitive to guanine nucleotides. When guanine nucleotides are incubated with unoccupied receptors, approximately 50% of the moderate affinity sites are apparently shifted to a

low affinity state such that they cannot be detected using the experimental protocols described. When Gpp(NH)p is introduced to occupied receptors, approximately 50% of the slow dissociating sites are apparently converted to fast dissociating sites. This conversion may characterize the stabilization of a low affinity state that accounts for the guanine nucleotide-induced loss of binding sites. The moderate affinity receptors might equilibrate to some extent with the low affinity state in the absence of guanine nucleotides, as suggested by the measurement of a fast dissociation rate in control membranes.

A major question arising from this study concerns the relation of receptor populations to the physiological effects of NPY at the cellular level. For example, physiological effects of NPY on neurons from brain and spinal cord include the following: 1) inhibition of voltage-sensitive inward Ca^{2+} current (30, 70, 71), 2) inhibition of neurotransmitter release (30, 32, 33, 39), 3) inhibition of adenylate cyclase activity (38, 72–74), 4) stimulation of inositol phosphate release (38, 69), 5) up-regulation of α_1-adrenergic receptors in the cerebral cortex (40), 6) regulation of α_2-adrenergic receptors in both the brainstem and the forebrain (35, 37, 41), and 7) potentiation of noradrenergic effects (32–34). Guanine nucleotide-binding proteins are proposed to be involved in at least the first five effects, and possibly the sixth as well (37). Thus, it seems likely that the guanine nucleotide-sensitive receptors mediate the majority of the documented effects. It may be that the function of the high affinity, guanine nucleotide-insensitive receptors will be elucidated by future studies. Alternatively, it is possible that the high affinity receptors are in the process of being added to or removed from the membrane and, as such, are not fully functional.

In conclusion, equilibrium and dissociation experiments suggest the existence of multiple NPY and PYY receptors in rat brain. The characterization of these apparent receptor populations will be facilitated by the development of receptor isolation and purification techniques.

References

1. Lundberg, J. M., L. Terenius, T. Hokfelt, and K. Tatemoto. Comparative immunohistochemical and biochemical analysis of pancreatic polypeptide-like peptides with special reference to the presence of neuropeptide Y in central and peripheral neurons. *J. Neurosci.* **4**:2376–2386 (1984).
2. Miyachi, Y., W. Jitsuishi, A. Miyoshi, S. Fujita, A. Mizuchi, and K. Tatemoto. The distribution of polypeptide YY-like immunoreactivity in rat tissues. *Endocrinology* **118**:2163–2167 (1986).
3. Schalling, M., K. Seroogy, T. Hokfelt, S. Y. Chai, H. Hallman, H. Persson, D. Larhammar, A. Ericsson, L. Terenius, J. Graffi, J. Massoulie, and M. Goldstein. Neuropeptide tyrosine in the rat adrenal gland: immunohistochemical and *in situ* hybridization studies. *Neuroscience* **24**:337–349 (1988).
4. Lukinius, A. I. C., J. L. E. Ericsson, M. K. Lundquist, and E. M. O. Wilander. Ultrastructural localization of serotonin and polypeptide YY (PYY) in endocrine cells of the human rectum. *J. Histochem. Cytochem.* **34**:719–726 (1986).
5. Broome, M., T. Hokfelt, and L. Terenius. Peptide YY (PYY)-immunoreactive neurons in the lower brainstem and spinal cord of rat. *Acta. Physiol. Scand.* **125**:349–352 (1985).
6. Ekman, R., C. Wahlestedt, G. Bottcher, R. Hakanson, and P. Panula. Peptide YY-like immunoreactivity in the central nervous system of the rat. *Regul. Peptides* **16**:157–168 (1986).
7. Tatemoto, K. Neuropeptide Y: complete amino acid sequence of the brain peptide. *Proc. Natl. Acad. Sci. USA* **79**:5485–5489 (1982).
8. Tatemoto, K., M. Carlquist, and V. Mutt. Neuropeptide Y: a novel brain peptide with structural similarities to peptide YY and pancreatic polypeptide. *Nature* (*Lond.*) **296**:659–660 (1982).
9. Lundberg, J. M., and K. Tatemoto. Pancreatic polypeptide family (APP, BPP, NPY and PYY) in relation to sympathetic vasoconstriction resistant to α-adrenoceptor blockade. *Acta Physiol. Scand.* **116**:393–402 (1982).
10. Zukowska-Grojec, Z., M. Haass, and M. A. Bayorh. Neuropeptide Y and peptide YY mediate nonadrenergic vasoconstriction and modulate sympathetic responses in rats. *Regul. Peptides* **15**:99–110 (1986).
11. Corder, R., P. J. Lowry, and P. G. Withrington. The actions of the peptides, neuropeptide Y and peptide YY, on the vascular and capsular smooth muscle of the isolated, blood perfused spleen of the dog. *Br. J. Pharmacol.* **90**:785–790 (1987).
12. Clark, J. T., A. Sahu, P. S. Kalra, A. Balasubramaniam, and S. P. Kalra. Neuropeptide Y (NPY)-induced feeding behavior in female rats: comparison with human NPY ([Met^{17}]), NPY analog ([norLeu^4]NPY) and peptide YY. *Regul. Peptides* **7**:31–39 (1987).
13. Kuenzel, W. J., L. W. Douglass, and B. A. Davison. Robust feeding following central administration of neuropeptide Y or peptide YY in chicks, *Gallus domesticus*. *Peptides* **8**:823–828 (1987).
14. Saria, A., and E. Beubler. Neuropeptide Y (NPY) and peptide YY (PYY) inhibit prostaglandin E_2-induced intestinal fluid and electrolyte secretion in the rat jejunum *in vivo*. *Eur. J. Pharmacol.* **119**:47–52 (1985).
15. Friel, D. D., R. J. Miller, and M. W. Walker. Neuropeptide Y: a powerful modulator of epithelial ion transport. *Br. J. Pharmacol.* **88**:425–431 (1986).
16. Cox, H. M., A. W. Cuthbert, R. Hakanson, and C. Wahlestedt. The effect of neuropeptide Y and peptide YY on electrogenic ion transport in rat intestinal epithelia. *J. Physiol.* (*Lond.*) **398**:65–80 (1988).
17. O'Donohue, T. L., B. M. Chronwall, R. M. Pruss, E. Mezey, J. Z. Kiss, L. E. Eiden, V. J. Massari, R. E. Tessel, V. M. Pickel, D. A. DiMaggio, A. J. Hotchkiss, W. R. Crowley, and Z. Zukowska-Grojec. Neuropeptide Y and peptide YY neuronal and endocrine systems. *Peptides* **6**:755–768 (1985).
18. Gray, T. S., and J. E. Morley. Neuropeptide Y: anatomical distribution and possible function in mammalian nervous system. *Life Sci.* **38**:389–401 (1986).
19. Laburthe, M., B. Chenut, C. Rouyer-Fessard, K. Tatemoto, A. Couvineau, A. Servin, and B. Amiranoff. Interaction of peptide YY with rat intestinal epithelial plasma membranes: binding of the radioiodinated peptide. *Endocrinology* **118**:1910–1917 (1986).
20. Inui, A., M. Oya, M. Okita, T. Inoue, N. Sakatani, H. Morioka, K. Shii, K. Yokono, N. Mizuno, and S. Baba. Peptide YY receptors in the brain. *Biochem. Biophys. Res. Commun.* **150**:25–32 (1988).
21. Edvinsson, L., E. Ekblad, R. Hakanson, and C. Wahlestedt. Neuropeptide Y potentiates the effect of various vasoconstrictor agents on rabbit blood vessels. *Br. J. Pharmacol.* **83**:519–525 (1984).
22. Wahlestedt, C., and R. Hakanson. Effects of neuropeptide Y (NPY) at the sympathetic neuroeffector junction: can pre- and postjunctional receptors be distinguished? *Med. Biol.* (*Helsinki*) **64**:85–88 (1986).
23. Wahlestedt, C., N. Yanaihara, and R. Hakanson. Evidence for different pre- and post-junctional receptors for neuropeptide Y and related peptides. *Regul. Peptides* **13**:307–318 (1986).
24. Lundberg, J. M., and L. Stjarne. Neuropeptide Y (NPY) depresses the secretion of ^{3}H-noradrenaline and the contractile response evoked by field stimulation in rat vas deferens. *Acta Physiol. Scand.* **120**:477–479 (1984).
25. Stjarne, L., J. M. Lundberg, and P. Astrand. Neuropeptide Y: a cotransmitter with noradrenaline and adenosine 5′-triphosphate in the sympathetic nerves of the mouse deferens? A biochemical, physiological and electropharmacological study. *Neuroscience* **18**:151–166 (1986).
26. Dahlof, C., P. Dahlof, and J. M. Lundberg. Neuropeptide Y (NPY): enhancement of blood pressure increase upon *alpha*-adrenoceptor activation and direct pressor effects in pithed rats. *Eur. J. Pharmacol.* **109**:289–292 (1985).
27. Pernow, J., A. Saria, and J. M. Lundberg. Mechanisms underlying pre- and post-junctional effects of neuropeptide Y in sympathetic vascular control. *Acta Physiol. Scand.* **126**:239–249 (1986).
28. Stjernquist, M., P. Emson, C. Owman, N.-O. Sjoberg, F. Sundler, and K. Tatemoto. Neuropeptide Y in the female reproductive tract of the rat: distribution of nerve fibres and motor effects. *Neurosci. Lett.* 39:279–284 (1983).
29. Potter, K. K. Prolonged non-adrenergic inhibition of cardiac vagal action following sympathetic stimulation: neuromodulation by neuropeptide Y? *Neurosci. Lett.* **54**:117–121 (1985).
30. Walker, M. W., D. A. Ewald, T. M. Perney, and R. J. Miller. Neuropeptide Y modulates neurotransmitter release and Ca^{2+} currents in rat sensory neurons. *J. Neurosci.* **8**:2438–2446 (1988).
31. Wahlestedt, C., L. Edvinsson, E. Ekblad, and R. Hakanson. Effects of neuropeptide Y at sympathetic neuroeffector junctions: existence of Y_1 and Y_2 receptors, in *Neuronal Messengers in Vascular Function* (A. Nobin and C. Owman, eds.). Fernstrom Symposium No. 10, in press.
32. Vacas, M. I., M. I. Keller Sarmiento, E. N. Pereyra, G. S. Etchegoyen, and D. P. Cardinali. *In vitro* effect of neuropeptide Y on melatonin and norepinephrine release in rat pineal gland. *Cell. Mol. Neurobiol.* **7**:309–315 (1987).
33. Yokoo, H., D. H. Schlesinger, and M. Goldstein. The effect of neuropeptide Y (NPY) on stimulation-evoked release of [^{3}H]norepinephrine (NE) from rat hypothalamic and cerebral cortical slices. *Eur. J. Pharmacol.* **143**:283–286 (1987).
34. Martire, M., K. Fuxe, G. Pistritto, P. Preziosi, and L. F. Agnati. Neuropeptide Y enhances the inhibitory effects of clonidine on ^{3}H-noradrenaline release in synaptosomes isolated from the medulla oblongata of the male rat. *J. Neural Transm.* **67**:114–124 (1986).
35. Agnati, L. F., K. Fuxe, F. Benfenati, N. Battistini, A. Harfstrand, K. Tatemoto, T. Hokfelt, and V. Mutt. Neuropeptide Y *in vitro* selectively increases the number of *alpha*$_2$-adrenergic binding sites in membranes of the medulla oblongata of the rat. *Acta Physiol. Scand.* **118**:293–295 (1983).
36. Fuxe, K., L. F. Agnati, A. Harfstrand, M. Martire, M. Goldstein, R. Grimaldi, P. Bernardi, I. Zini, K. Tatemoto, and V. Mutt. Evidence for a modulation by neuropeptide Y of the *alpha*-adrenergic transmission line in central adrenaline synapses: new possibilities for treatment of hypertensive disorders. *Clin. Exp. Hypertens.* **[A]6**(10&11):1951–1956 (1984).
37. Fuxe, K., A. Harfstrand, L. F. Agnati, M. Kalia, B. Fredholm, T. Svensson, J.-A. Gustafsson, R. Lang, and D. Ganten. Central catecholamine-neuropep-

tide Y interactions at the pre- and post-synaptic level in cardiovascular centers. *J. Cardiovasc. Pharmacol.* **10**(suppl. 12):S1-S13 (1987).
38. Wahlestedt, C., P. Siminsson, A. Westlind-Danielsson, T. Bartfai, and R. Hakanson. Neuropeptide Y receptor sub-types are coupled to different second messengers, in *Neuropeptide Y (NPY): Actions and Interactions in Neurotransmission.* C. Wahlestedt, Ph.D. dissertation, University of Lund, Sweden (1987).
39. Ciarleglio, A. E., M. C. Beinfeld, and T. C. Westfall. Effect of neuropeptide Y on the release of [^{3}H]-norepinephrine from the anterior hypothalamus and nucleus of the solitary tract region of rats. *Soc. Neurosci. Abstr.* **12**:1006 (1986).
40. Wahlestedt, C., P. Persson, M. Heilig, E. Rosengren, and R. Hakanson. Studies on interactions between neuropeptide Y (NPY) and noradrenaline in rat cerebral cortex, in *Neuropeptide Y (NPY): Actions and Interactions in Neurotransmission.* Wahlestedt, Ph.D. dissertation, University of Lund, Sweden (1987).
41. Unnerstall, J. R., T. A. Kopajtic, and H. L. Loats. Differential effects of neuropeptide Y on the binding of *alpha*$_2$ adrenergic agonists and antagonists in the rat forebrain. *Soc. Neurosci. Abstr.* **12**:415 (1986).
42. Unden, A., K. Tatemoto, V. Mutt, and T. Bartfai. Neuropeptide Y receptor in the rat brain. *Eur. J. Biochem.* **125**:525–530 (1984).
43. Unden, A., and T. Bartfai. Regulation of neuropeptide Y (NPY) binding by guanine nucleotides in the rat cerebral cortex. *FEBS Let.* **177**:125–128 (1984).
44. Saria, A., E. Theodorsson-Norheim, and J. M. Lundberg. Evidence for specific neuropeptide Y-binding sites in rat brain synaptosomes. *Eur. J. Pharmacol.* **107**:105–107 (1985).
45. Chang, R. S. L., V. J. Lotti, T.-B. Chen, D. J. Cerino, and P. J. Kling. Neuropeptide Y (NPY) binding sites in rat brain labeled with ^{125}I-Bolton-Hunter NPY: comparative potencies of various polypeptides on brain NPY binding and biological responses in rat vas deferens. *Life Sci.* **37**:2111–2122 (1985).
46. Chang, R. S. L., V. J. Lotti, and T.-B. Chen. Increased neuropeptide Y (NPY) receptor binding in hippocampus and cortex of spontaneous hypertensive (SH) rats compared to normotensive (WKY) rats. *Neurosci. Lett.* **67**:275–278 (1986).
47. Goldstein, M., N. Kusano, C. Adler, and E. Meller. Characterization of central neuropeptide Y receptor binding sites and possible interactions with *alpha*$_2$-adrenoceptors. *Prog. Brain Res.* **68**:331–335 (1986).
48. Martel, H.-C., S. St.-Pierre, P. J. Bedard, and R. Quirion. Comparison of [^{125}I]Bolton-Hunter neuropeptide Y binding sites in the forebrain of various mammalian species. *Brain Res.* **419**:403–407 (1987).
49. Nakajima, T., Y. Yashima, and K. Nakamura. Quantitative autoradiographic localization of neuropeptide Y receptors in the rat lower brainstem. *Brain Res.* **380**:144–150 (1986).
50. Nakajima, T., Y. Yashima, and K. Nakamura. Higher density of ^{125}I-neuropeptide Y receptors in the area postrema of SHR. *Brain Res.* **417**:360–362 (1987).
51. Martel, J.-C., S. St.-Pierre, and R. Quirion. Neuropeptide Y neurotransmitter in rat brain: autoradiographic localization. *Peptides* **7**:55–60 (1986).
52. Bradford, M. M.: A rapid and sensitive method for the quantitation of microgram quantities of protein utilizing the principle of protein-dye binding. *Anal. Biochem.* **72**:248–254 (1976).
53. Yamaoka, K., Y. Tanigawara, T. Nakagawa, and T. Uno. A pharmacokinetic analysis program (multi) for microcomputer. *J. Pharmacobio-Dyn.* **4**:879–885 (1981).
54. Nelder, J. A., and R. Mead. A simplex method for function minimization. *Comput. J.* **7**:308–313 (1965).
55. Draper, N. R., and H. Smith. *Applied Regression Analysis.* Wiley, New York (1966).
56. Allen, J. M., J. Hughes, and S. R. Bloom. Presence, distribution, and pharmacological effects of neuropeptide Y in mammalian gastrointestinal tract. *Dig. Dis. Sci.* **32**:506–512 (1987).
57. Wahlestedt, C., L. Grundemar, and R. Hakanson. PYY 13–36 reduces blood pressure in the rat unlike NPY and PYY, in *Neuropeptide Y (NPY): Actions and Interactions in Neurotransmission.* C. Wahlestedt, Ph.D. dissertation, University of Lund, Sweden (1988).
58. Lundberg, J. M., A. Hemsen, O. Larsson, A. Rudehill, A. Saria, and B. B. Fredholm. Neuropeptide Y receptor in pig spleen: binding characteristics, reduction of cyclic AMP formation and calcium antagonists inhibition of vasconstriction. *Eur. J. Pharmacol.* **145**:21–29 (1988).
59. Rioux, F., H. Bachelard, J.-C. Martel, and S. St.-Pierre. The vasoconstrictor effect of neuropeptide Y and related peptides in the guinea pig isolated heart. *Peptides* **7**:27–31 (1986).
60. Schwartz, T. W., S. P. Sheikh, and M. M. T. O'Hare. Receptors on phaeochromocytoma cells for two members of the PP-fold family—NPY and PP. *FEBS Lett.* **225**:209–214 (1987).
61. Enjalbert, A., R. Rasolonjanahary, E. Moyse, C. Kordon, and J. Epelbaum. Guanine nucleotide sensitivity of [^{125}I]-iodo-*N*-Tyr-somatostatin binding in rat adenohypophysis and cerebral cortex. *Endocrinology* **113**:822–824 (1983).
62. Lee, C. M., J. A. Javitch, and S. H. Snyder. ^{3}H-Substance P binding to salivary gland membranes: regulation by guanyl nucleotides and divalent cations. *Mol Pharmacol.* **23**:563–569 (1983).
63. Glover, I., I. Haneef, J. Pitts, S. Wood, D. Moss, I. Tickle, and T. Blundell. Conformational flexibility in a small globular hormone: X-ray analysis of avian pancreatic polypeptide at 0.98 Å resolution. *Biopolymers* **22**:293–304 (1983).
64. Glover, I. D., D. J. Barlow, J. W. Pitts, S. P. Wood, I. J. Tickle, T. L. Blundell, J. Tatemoto, J. Kimmel, A. Wollmer, W. Strassburger, and Y. Zhang. Conformation studies on the pancreatic polypeptide hormone family. *Eur. J. Biochem.* **142**:379–385 (1985).
65. Wood, S. P., J. E. Pitts, T. L. Blundell, I. J. Tickle, and J. A. Jenkins. Purification, crystallization and preliminary X-ray studies in avian pancreatic polypeptide. *Eur. J. Biochem.* **78**:119–126 (1977).
66. Blundell, T. L., J. E. Pitts, I. J. Tickle, S. P. Wood, and C.-W. Wu. X-ray analysis (1.4 Å resolution) of avian pancreatic polypeptide: small globular protein hormone. *Proc. Natl. Acad. Sci. USA* **78**:4175–4179 (1981).
67. Krstenansky, J. L., and S. H. Buck. The synthesis, physical characterization and receptor binding affinity of neuropeptide Y (NPY). *Neuropeptides* **10**:77–85 (1987).
68. Allen, J., J. Novotny, J. Martin, and G. Heinrich. Molecular structure of mammalian neuropeptide Y: analysis by molecular cloning and computer-aided comparison with crystal structure of avian homologue. *Proc. Natl. Acad. Sci. USA* **84**:2532–2536 (1987).
69. Perney, T. M., and R. J. Miller. Neurotransmitter regulation of lipid metabolism in cultured rat sensory neurons. *Soc. Neurosci. Abstr.* **13**:1135 (1987).
70. Colmers, W. F., K. Lukowiak, and Q. J. Pittman. Neuropeptide Y reduces orthodromically evoked population spike in rat hippocampal CA1 by a possibly presynaptic mechanism. *Brain Res.* **346**:404–408 (1985).
71. Colmers, W. F., K. Lukowiak, and Q. J. Pittman. Presynaptic action of neuropeptide Y in area CA1 of the rat hippocampal slice. *J. Physiol.* (*Lond.*) **383**:285–299 (1987).
72. Harfstrand, A., B. Fredholm, and K. Fuxe. Inhibitory effects of neuropeptide Y on cyclic AMP accumulation in slices of the nucleus tractus solitarius region of the rat. *Neurosci. Lett.* **76**:185–190 (1987).
73. Petrenko, S., M. C. Olianas, P. Onali, and G. L. Gessa. Neuropeptide Y inhibits forskolin-stimulated adenylate cyclase activity in rat hippocampus. *Eur. J. Pharmacol.* **136**:425–428 (1987).
74. Westlind-Danielsson, A., A. Andell, J. Abens, and T. Bartfai. Neuropeptide Y and peptide YY inhibit adenylate cyclase activity in the rat striatum. *Acta Physiol. Scand.* **132**:425–430 (1988).

Send reprint requests to: Richard J. Miller, Ph.D., Dept. Pharmacological and Physiological Sciences, University of Chicago, 947 East 58th Street, Chicago IL 60637.